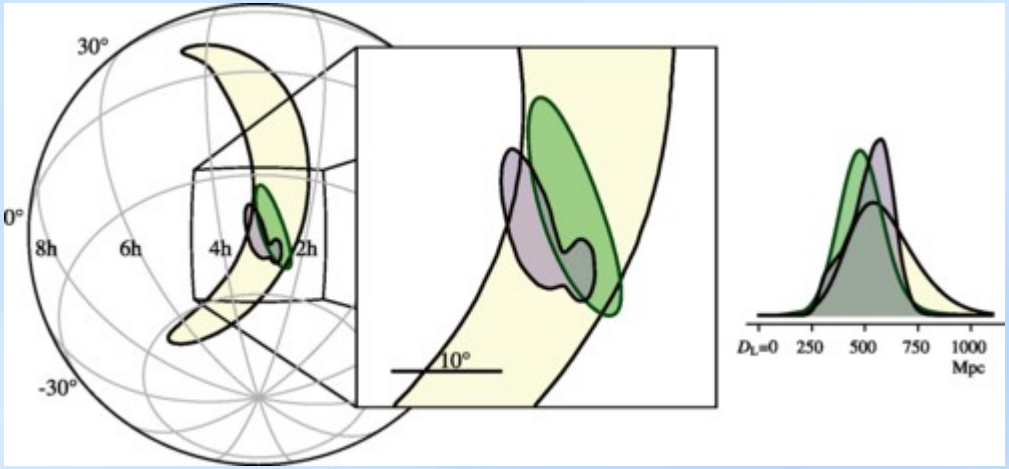

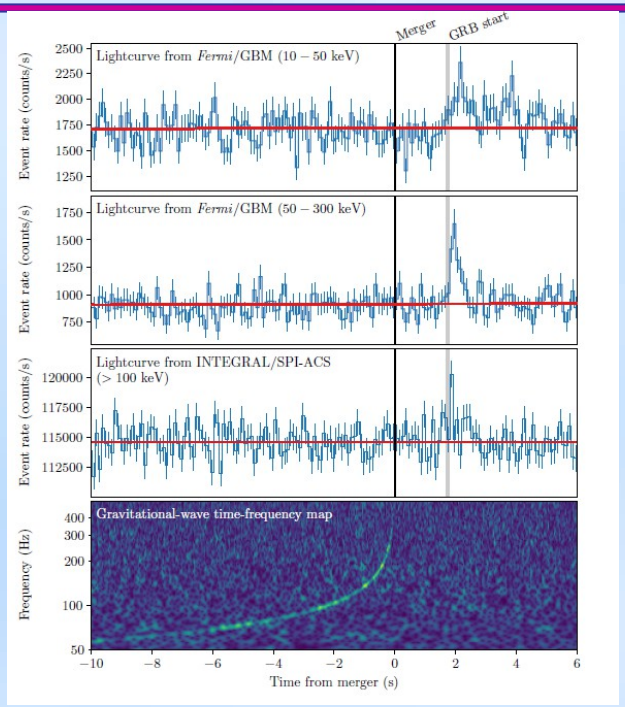

Gravitational Waves – Data Science Meetup

Nelson Christensen for Artemis
Observatoire de la Côte d'Azur, Nice

General Relativity

1915: Einstein's Theory of General Relativity

1916: Einstein paper on linear approximation to general relativity with multiple applications, including gravitational waves.

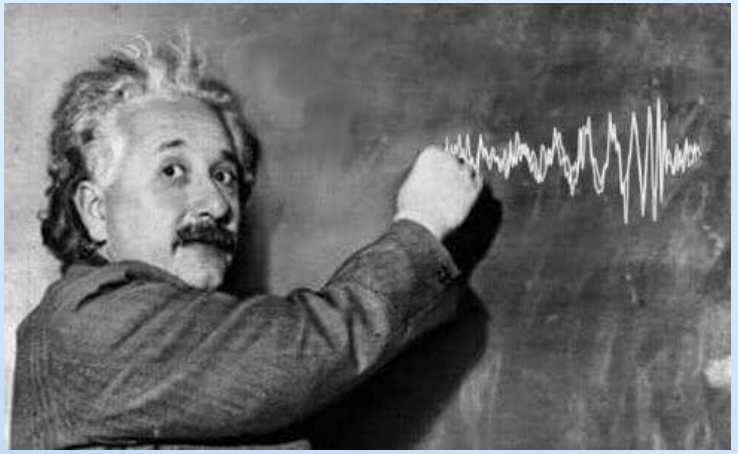

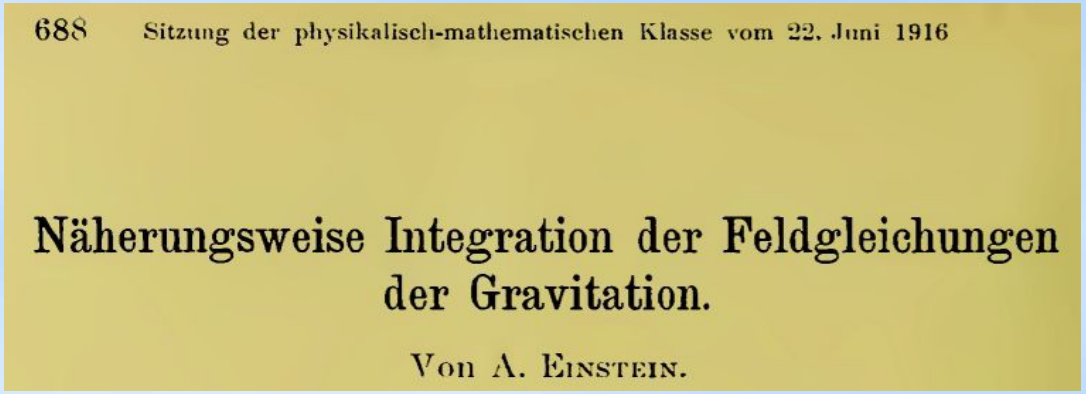

688 Sitzung der physikalisch-mathematischen Klasse vom 22. Juni 1916

Näherungsweise Integration der Feldgleichungen der Gravitation.

Von A. Einstein.

Approximative Integration of the Field Equations of Gravitation

Gravitational Waves

$$A = \frac{\varkappa}{24\pi} \sum_{\alpha\beta} \left(\frac{\partial^3 J_{\alpha\beta}}{\partial t^3} \right)^2 . \qquad (21)$$

Würde man die Zeit in Sekunden, die Energie in Erg messen, so würde zu diesem Ausdruck der Zahlenfaktor $\frac{1}{c^4}$ hinzutreten. Berücksichtigt man außerdem, daß $\varkappa = 1.87 \cdot 10^{-27}$, so sieht man, daß A in allen nur denkbaren Fällen einen praktisch verschwindenden Wert haben muß.

"… in all conceivable cases, ***A*** must have a practically vanishing value."

Gravitational waves are predicted by Einstein, but he recognizes that they are too small.

Gravitational Waves

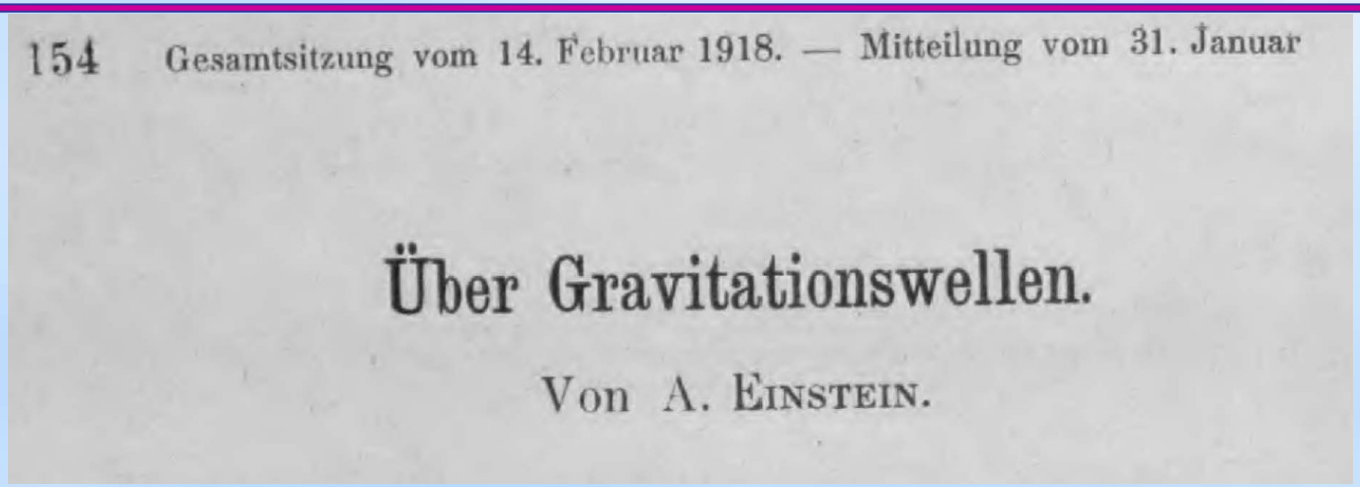

154 Gesamtsitzung vom 14. Februar 1918. — Mitteilung vom 31. Januar

Über Gravitationswellen.

Von A. Einstein.

On Gravitational Waves – 1918

Einstein works out the remaining details on gravitational waves: emission (quadrupole), polarizations, they carry energy, etc

Dabei ist zur Abkürzung

$$\mathfrak{J}_{\mu\nu} = \int x_\mu x_\nu \rho \, dV_0 \qquad (23)$$

gesetzt; $\mathfrak{J}_{\mu\nu}$ sind die Komponenten des (zeitlich variabeln) Trägheitsmomentes des materiellen Systems.

$$\gamma'_{23} = -\frac{\varkappa}{4\pi R} \ddot{\mathfrak{J}}_{23}.$$

While we are at it … Black Holes!

Über das Gravitationsfeld eines Massenpunktes nach der Einsteinschen Theorie.

Von K. Schwarzschild.

(Vorgelegt am 13. Januar 1916 [s. oben S. 42].)

On the gravitational field of a mass point according to Einstein's theory

$$ds^2 = (1 - \alpha/R)\,dt^2 - \frac{dR^2}{1 - \alpha/R} - R^2(d\vartheta^2 + \sin^2\vartheta\, d\phi^2),\quad R = (r^3 + \alpha^3)^{1/3}. \quad (14)$$

Dasselbe enthält die eine Konstante α, welche von der Größe der im Nullpunkt befindlichen Masse abhängt.

The concept of a “Black Hole” was not recognized by Schwarzschild:
A. Eddington 1924, G. Lemaître 1933, R. Oppenheimer 1939, D. Finkelstein 1958, …

What Are Gravitational Waves?

- General relativity (1916) prediction.
- Gravity is not really a force in GR, but a space-time deformation.
- Masses locally deform space-time.
- Accelerated masses emit gravitational waves, ripples in space time.
- Space-time is rigid:

  The amplitude of the deformation is tiny.

  Need cataclysmic events in order to expect to measure something on Earth … $h \sim 10^{-21}$

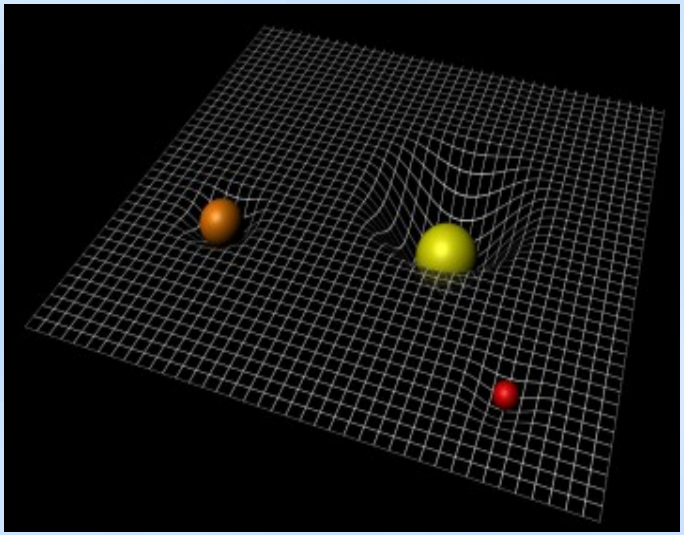

- Gravitational Wave sources: mainly astrophysical in the 10 Hz -10 kHz bandwidth

Gravitational Waves

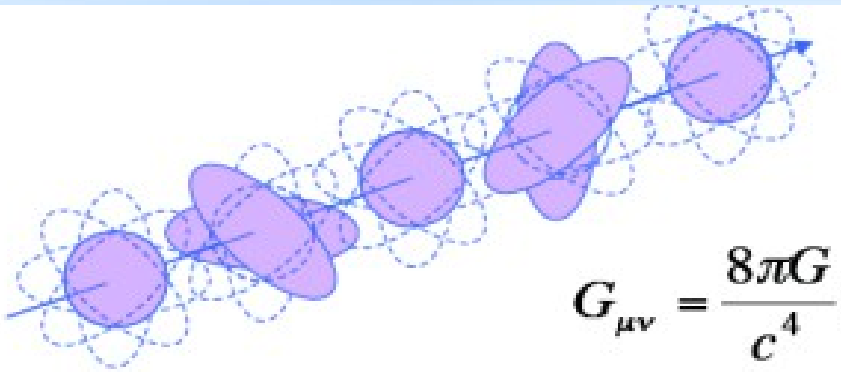

Gravitational waves are quadrupolar distortions of distances between freely falling masses. They are produced by time-varying mass quadrupoles.

$$G_{\mu\nu} = \frac{8\pi G}{c^4} T_{\mu\nu} \; (= 0 \text{ in vacuum})$$

$$h_{\mu\nu} \sim \frac{2G}{c^4 r} \ddot{I}_{\mu\nu}$$

$$g_{\mu\nu} = \eta_{\mu\nu} + h_{\mu\nu} \qquad h = 2\frac{\Delta L}{L}$$

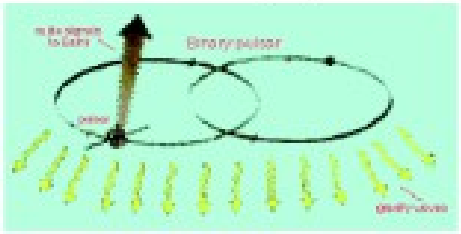

$$h_{\mu\nu} \sim \frac{R_1 R_2}{Dr}$$

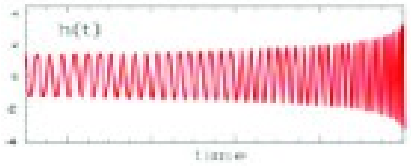

GWs from a NS-NS coalescence in the Virgo cluster has $h \sim 10^{-21}$ near Earth: change the distance between the Sun and the Earth by ~ one atomic diameter, and change 1km distance by ~10^{-18} m. They happen ~once every 50 years.

Effect Of A Gravitational Wave

"+" polarization:

$$h_+(t-z) = h^{TT}_{xx} = -h^{TT}_{yy}$$

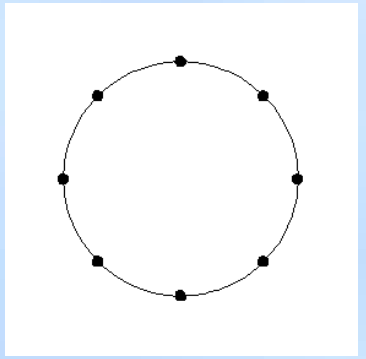

"x" polarization:

$$h_\times(t-z) = h^{TT}_{xy} = h^{TT}_{yx}$$

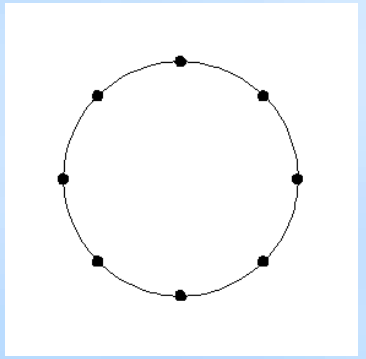

$$\frac{\Delta L}{L} = \frac{h}{2}$$ "strain"

Are Gravitational Waves Real?

Continued debate on whether gravitational waves really exist up until 1957 Chapel Hill conference.

Felix Pirani paper and presentation: relative acceleration of particle pairs can be associated with the Riemann tensor. The interpretation of the attendees was that non-zero components of the Riemann tensor were due to gravitational waves.

Sticky bead (Felix Pirani, Richard Feynman, Hermann Bondi)

Joe Weber of the University of Maryland, and from this inspiration started to think about gravitational wave detection.

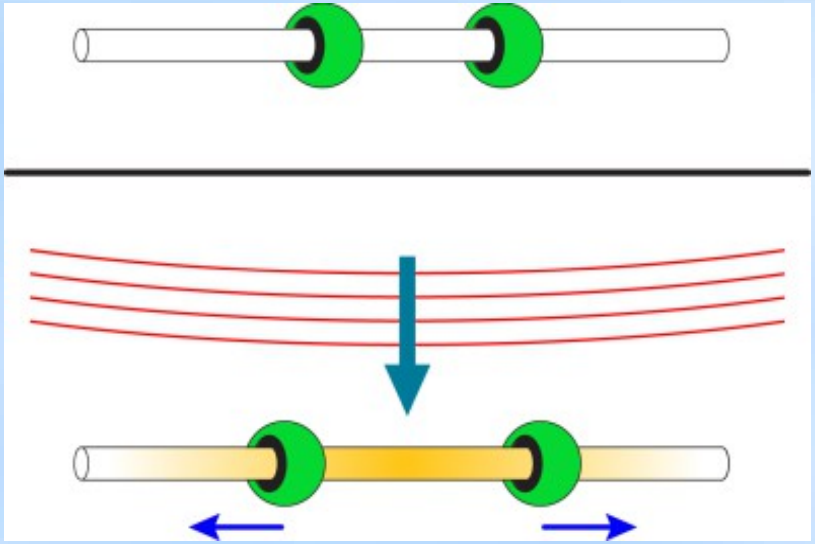

Gravitational Wave Detection

Inspired and motivated by the Chapel Hill Conference, Joe Weber of the University of Maryland constructs the first gravitational wave detectors.

"In 1958 I was able to prove, using Einstein's equations that a gravitational wave would change the dimensions of an extended body."

Binary Pulsar PSR 1913+16

M1 = 1.438 M_o

M2 = 1.390 M_o

8 hour orbit
Orbit decays by 3mm per orbit.

Discovered in 1974 by Russell Hulse and Joseph Taylor, then at University Massachusetts.

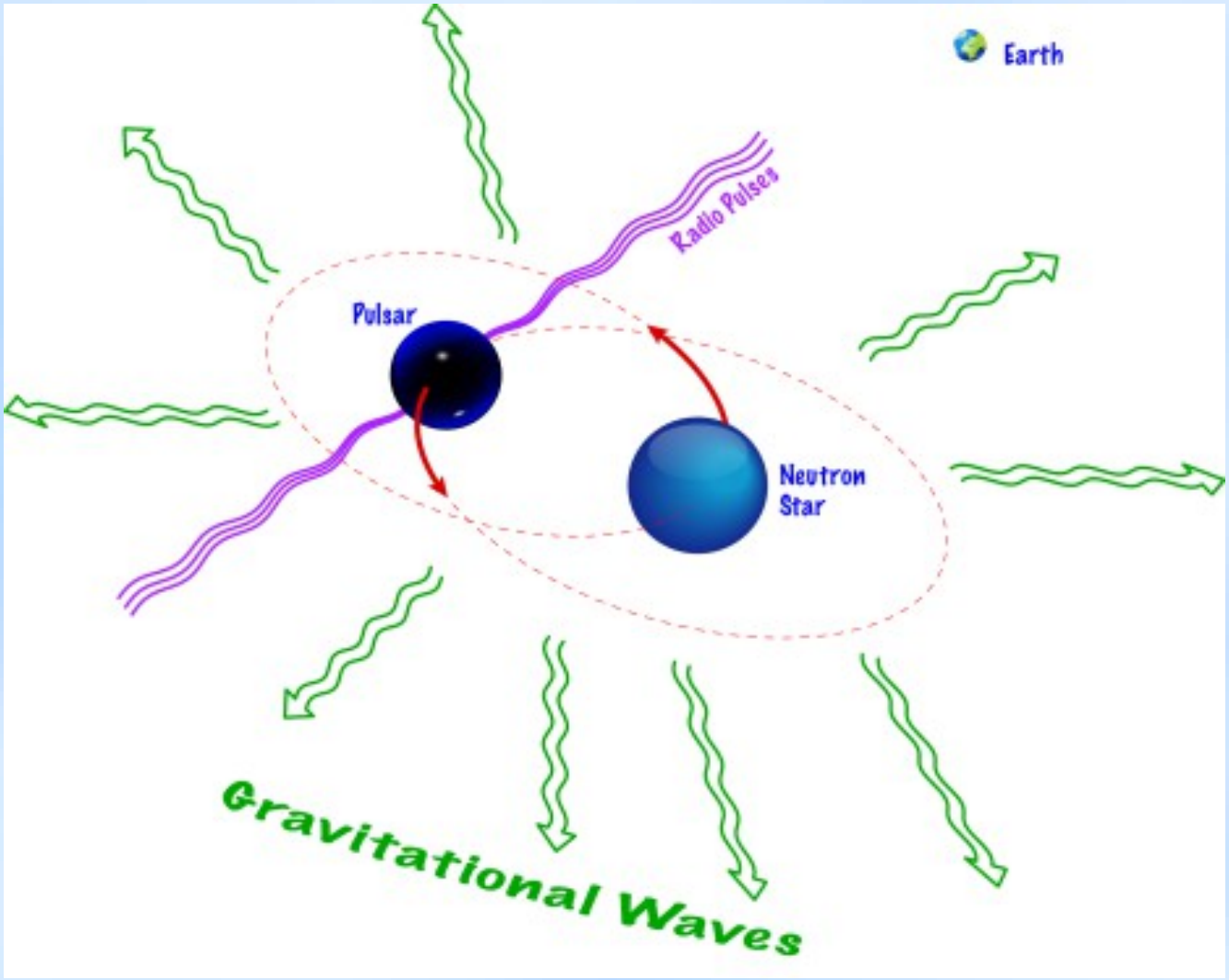

First Proof That Gravitational Waves Exist - 1982

THE ASTROPHYSICAL JOURNAL, 253:908–920, 1982 February 15

A NEW TEST OF GENERAL RELATIVITY: GRAVITATIONAL RADIATION AND THE BINARY PULSAR PSR 1913+16

J. H. TAYLOR AND J. M. WEISBERG
Department of Physics and Astronomy, University of Massachusetts, Amherst; and Joseph Henry Laboratories, Physics Department, Princeton University
Received 1981 July 2; accepted 1981 August 28

ABSTRACT

Observations of pulse arrival times from the binary pulsar PSR 1913+16 between 1974 September and 1981 March are now sufficient to yield a solution for the component masses and the absolute size of the orbit. We find the total mass to be almost equally distributed between the pulsar and its unseen companion, with $m_p = 1.42 \pm 0.06\ M_\odot$ and $m_c = 1.41 \pm 0.06\ M_\odot$. These values are used, together with the well determined orbital period and eccentricity, to calculate the rate at which the orbital period should decay as energy is lost from the system via gravitational radiation. According to the general relativistic quadrupole formula, one should expect for the PSR 1913+16 system an orbital period derivative $\dot{P}_b = (-2.403 \pm 0.005) \times 10^{-12}$. Our observations yield the measured value $\dot{P}_b = (-2.30 \pm 0.22) \times 10^{-12}$. The excellent agreement provides compelling evidence for the existence of gravitational radiation, as well as a new and profound confirmation of the general theory of relativity.

Subject headings: gravitation — pulsars — relativity

Gravitational Wave Proof

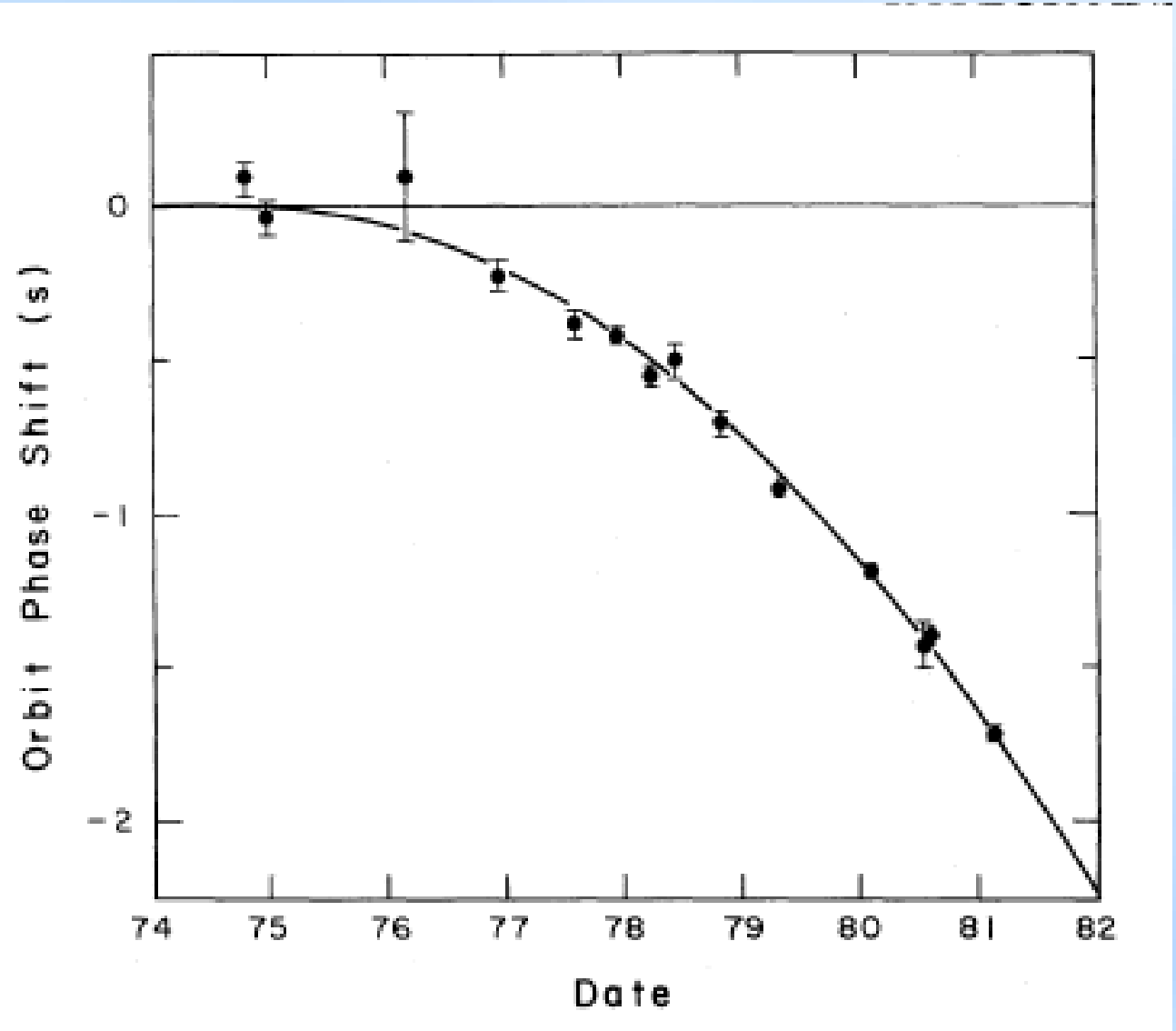

Taylor and Weisberg, 1982

Binary Pulsar Studies Continue

The Astrophysical Journal, 829:55 (10pp), 2016 September 20
doi:10.3847/0004-637X/829/1/55

RELATIVISTIC MEASUREMENTS FROM TIMING THE BINARY PULSAR PSR B1913+16

J. M. Weisberg and Y. Huang
Department of Physics and Astronomy, Carleton College, Northfield, MN 55057, USA; jweisber@carleton.edu
Received 2016 January 19; revised 2016 April 20; accepted 2016 June 1; published 2016 September 21

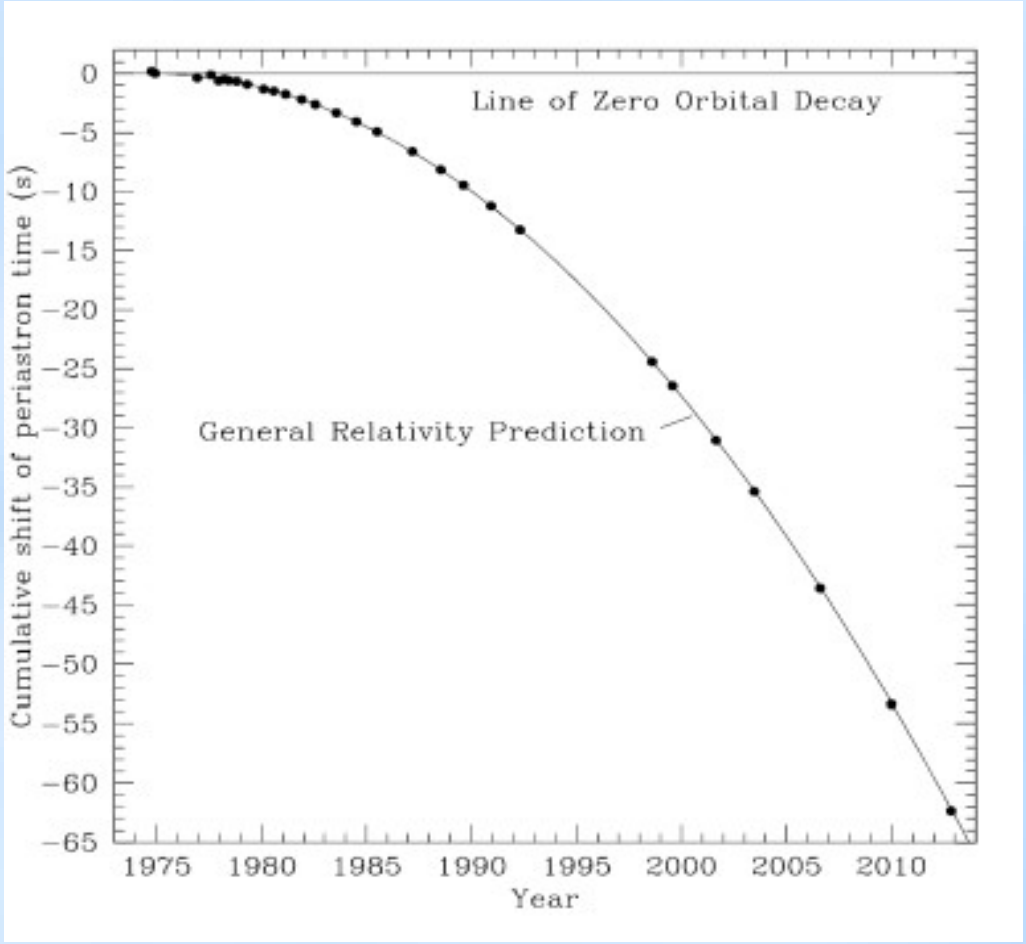

"The points, with error bars too small to show, represent our measurements"

The Detectors

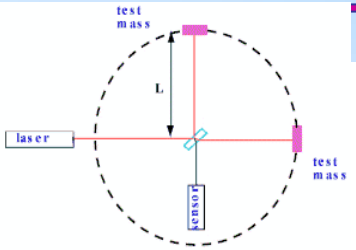

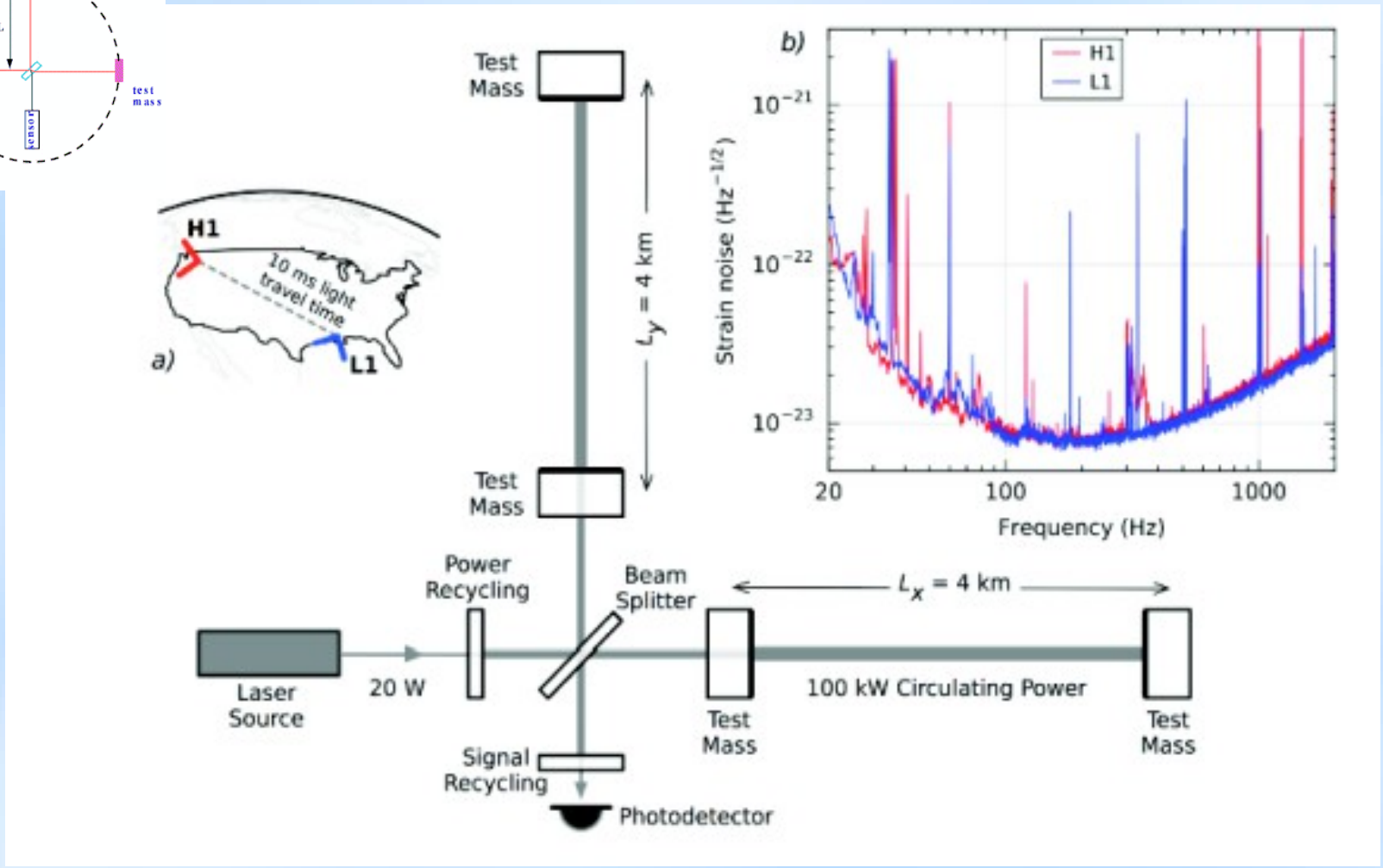

Advanced LIGO – Advanced Virgo

Livingston, Louisiana, USA

Hanford, Washington, USA

Cascina, Pisa, Italy

Advanced LIGO – Advanced Virgo

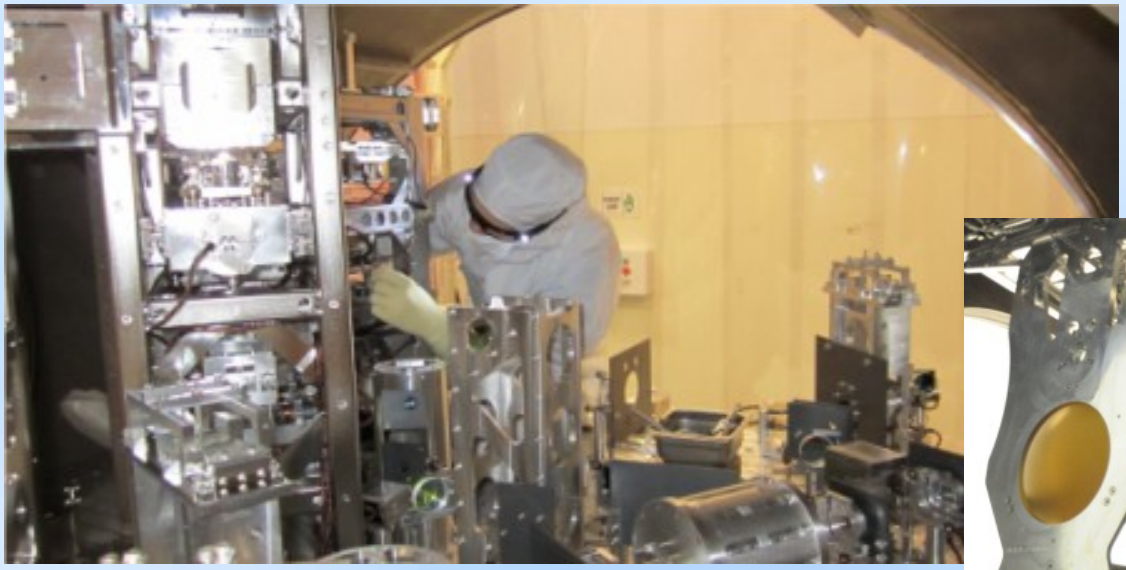

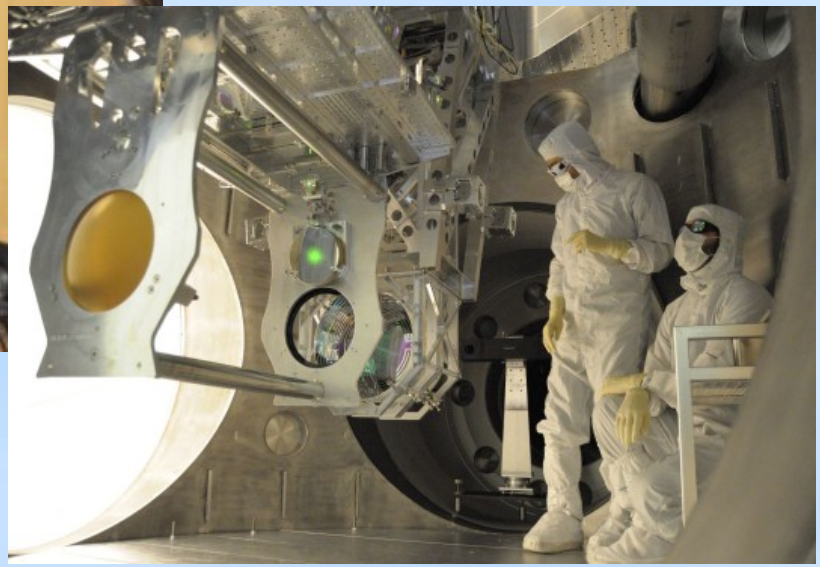

Built on the experience gained from the first generation detectors

Advanced LIGO

- Initial LIGO: 2005-2010.
- Advanced LIGO commissioned 2010-2015.
  - » Increased laser power
  - » Sophisticated seismic/vibration suppression
  - » Quadruple pendula suspensions
  - » Larger mirrors, better suspension material
  - » More complex and versatile interferometer configuration.

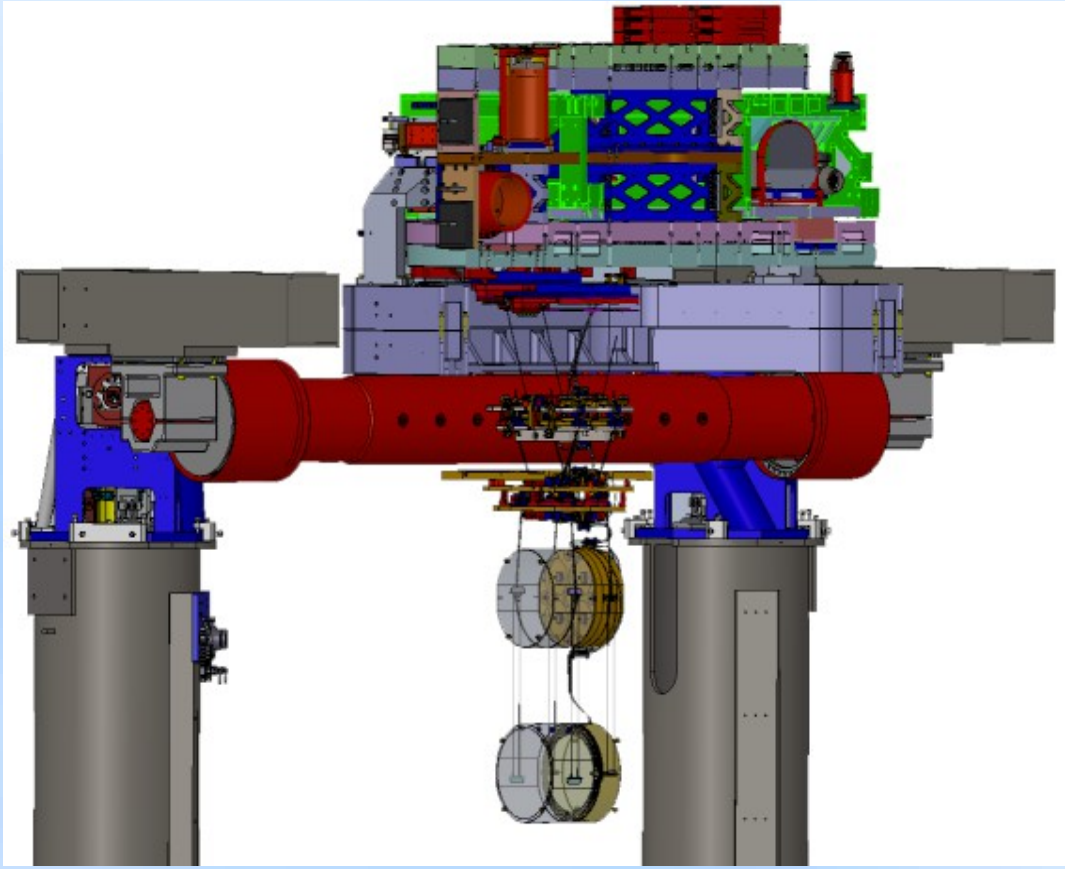

Classical and Quantum Gravity 32, 074001 (2015)

Virgo

Vue aérienne du site en cours de construction près de Cascina (Italie)

- Constructions starts 1996, Cascina, next to Pisa.
- 2003 Construction finishes
- 2007 – Memorandum of Understanding with LIGA
- 2007-2011 Initial Virgo scientific runs with LIGO
- 2011 – 2017 Upgrade to Advanced Virgo
- August 2017 Advanced Virgo joins observing run O2 with Advanced LIGO

Advanced Virgo

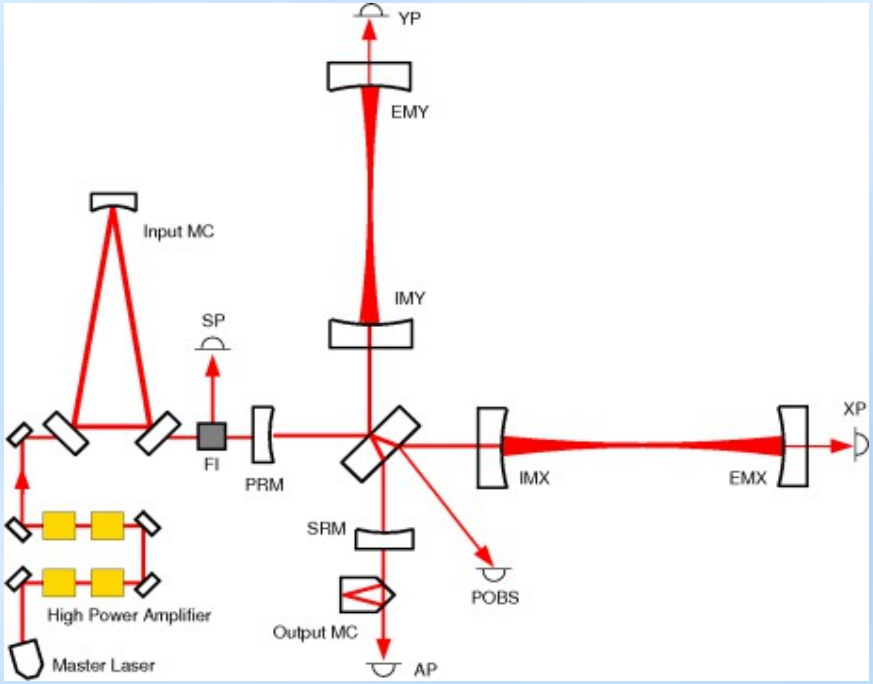

- Larger mirrors; better optical quality.
- Higher finesse of the arm cavities
- Increased laser power.
- Came on-line August 2017.

Advanced Virgo

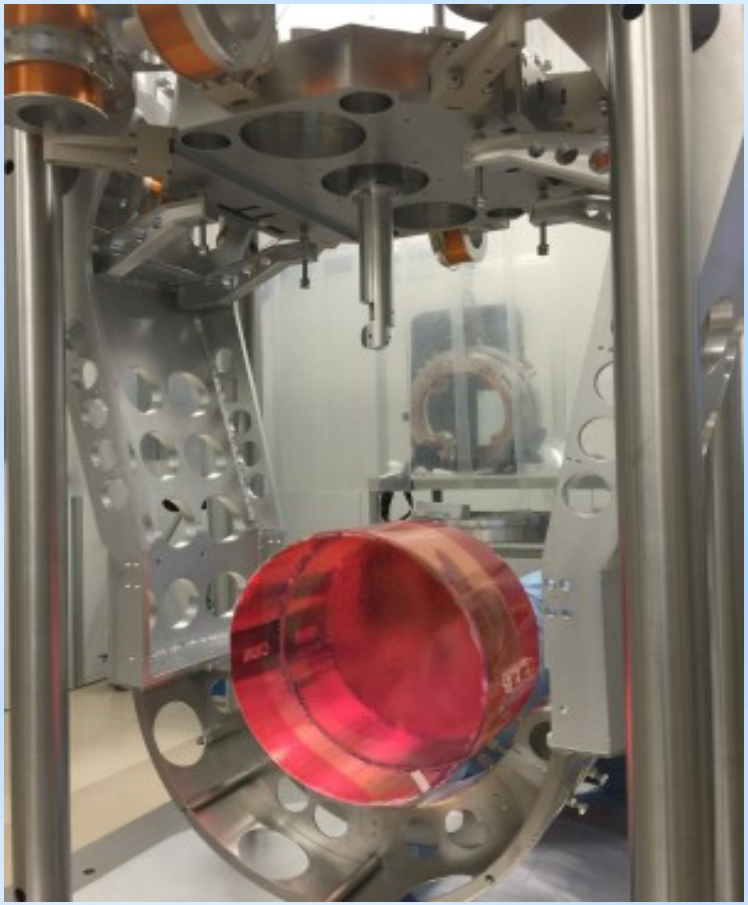

Mirror

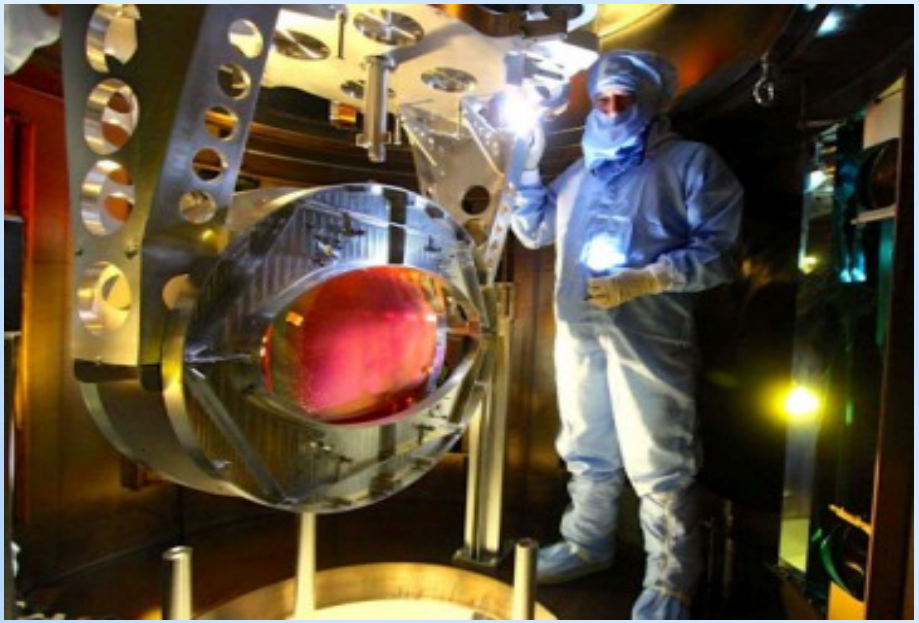

Beamsplitter

The optical components are very large, but their quality is exquisite.

GW150914

- Band-pass filter:
  35-350 Hz
- L1-H1 time delay of about 7ms.
- Chirp signal, typical of binary coalescences.
- Detected by online burst search pipelines.
- Confirmed later matched template searches.
- Combined SNR: 24.

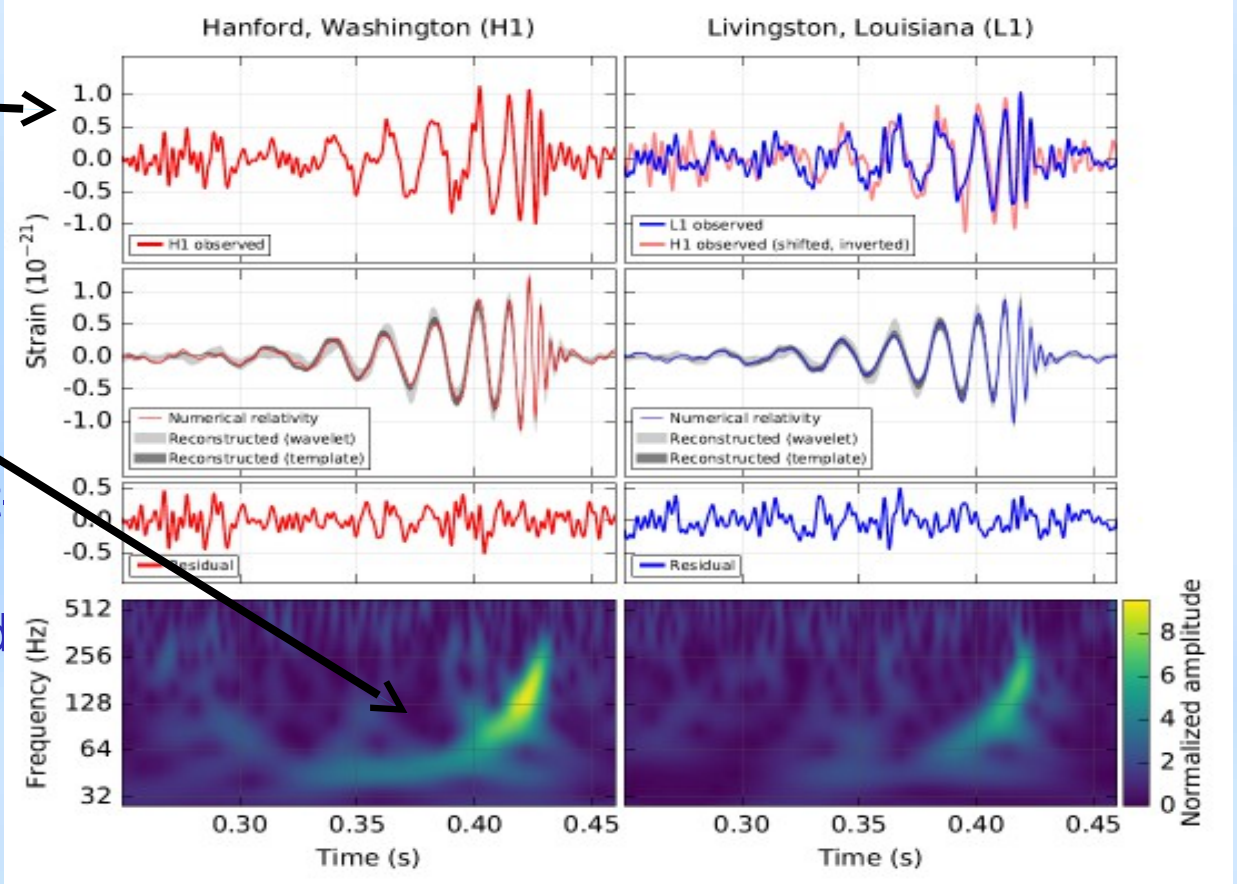

The Results

Observation of Gravitational Waves from a Binary Black Hole Merger

B. P. Abbott *et al.*[*]
(LIGO Scientific Collaboration and Virgo Collaboration)
(Received 21 January 2016; published 11 February 2016)

On September 14, 2015 at 09:50:45 UTC the two detectors of the Laser Interferometer Gravitational-Wave Observatory simultaneously observed a transient gravitational-wave signal. The signal sweeps upwards in frequency from 35 to 250 Hz with a peak gravitational-wave strain of 1.0×10^{-21}. It matches the waveform predicted by general relativity for the inspiral and merger of a pair of black holes and the ringdown of the resulting single black hole. The signal was observed with a matched-filter signal-to-noise ratio of 24 and a false alarm rate estimated to be less than 1 event per 203 000 years, equivalent to a significance greater than 5.1σ. The source lies at a luminosity distance of 410^{+160}_{-180} Mpc corresponding to a redshift $z = 0.09^{+0.03}_{-0.04}$. In the source frame, the initial black hole masses are $36^{+5}_{-4}M_{\odot}$ and $29^{+4}_{-4}M_{\odot}$, and the final black hole mass is $62^{+4}_{-4}M_{\odot}$, with $3.0^{+0.5}_{-0.5}M_{\odot}c^2$ radiated in gravitational waves. All uncertainties define 90% credible intervals. These observations demonstrate the existence of binary stellar-mass black hole systems. This is the first direct detection of gravitational waves and the first observation of a binary black hole merger.

DOI: 10.1103/PhysRevLett.116.061102

Primary black hole mass	$36^{+5}_{-4}M_{\odot}$
Secondary black hole mass	$29^{+4}_{-4}M_{\odot}$
Final black hole mass	$62^{+4}_{-4}M_{\odot}$
Final black hole spin	$0.67^{+0.05}_{-0.07}$
Luminosity distance	410^{+160}_{-180} Mpc
Source redshift z	$0.09^{+0.03}_{-0.04}$

A Century Of Theoretical Developments

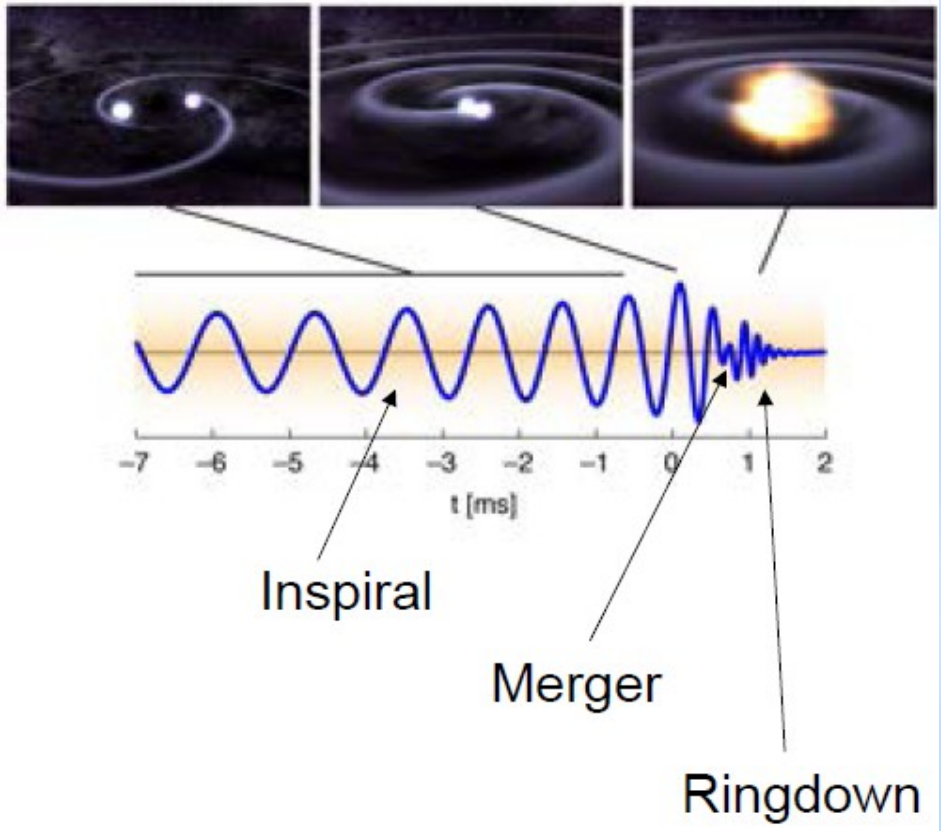

Sources: Compact Binary Coalescence

- Compact binary objects:
  - » Two neutron stars and/or black holes.
- Inspiral toward each other.
  - » Emit gravitational waves as they inspiral.
- Amplitude and frequency of the waves increases over time, until the merger.
- Waveform relatively well understood, matched template searches.

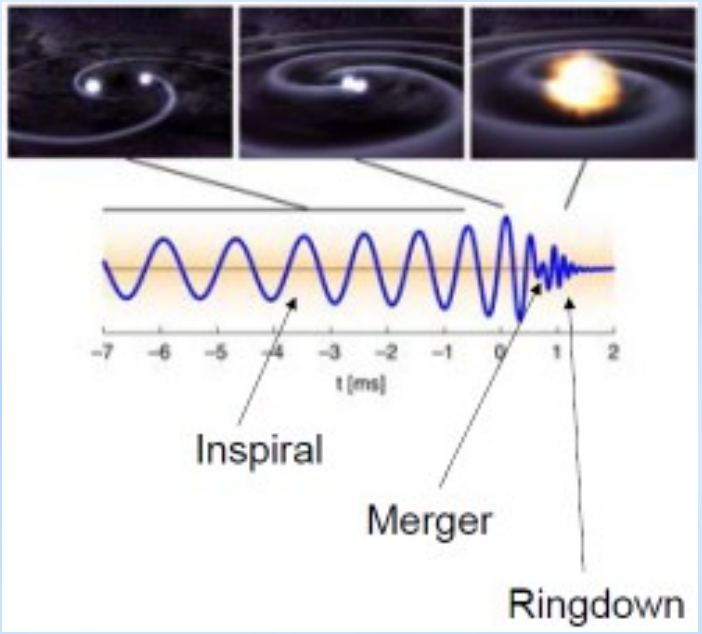

Matched Filtering and Time Slides

Spinning binary systems

Non-spinning components

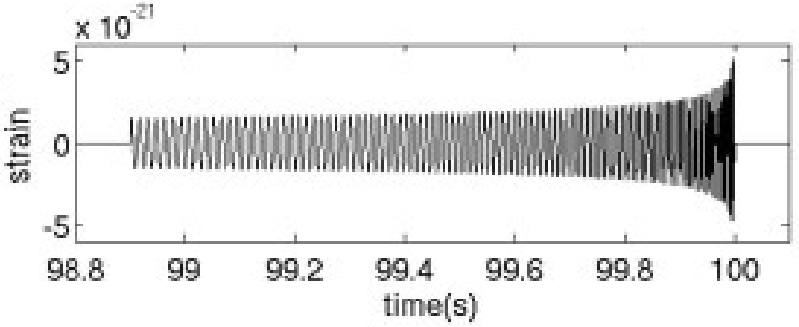

Spinning components

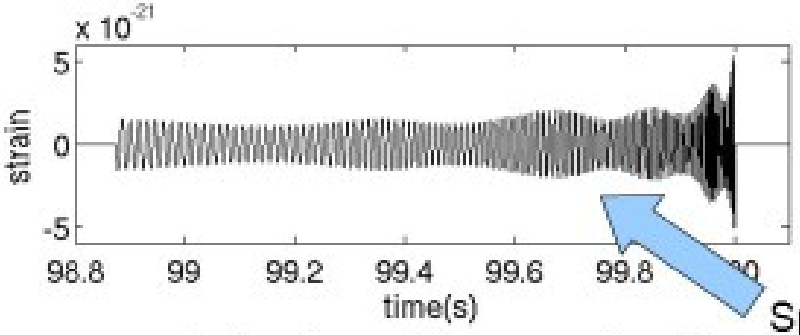

Spin modulation

- Waveforms generated using PN approximations
- Require up to 17 physical parameters
- Spin-orbit and spin-spin coupling (2PN)

LIGO-G070430-00-Z

Amaldi 2007

Matched Filtering and Time Slides

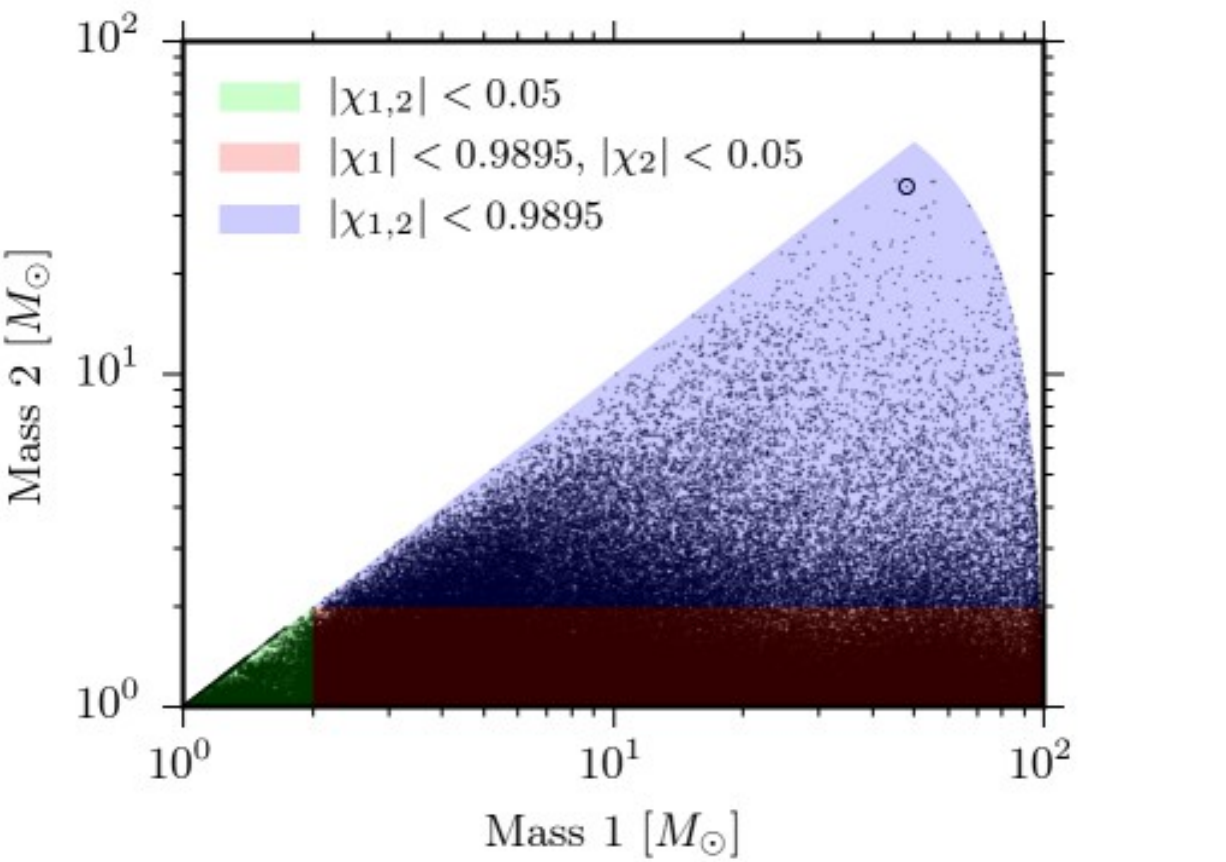

Search for signals, varying mass and spin of objects, for all times.

GW151226 – A Success For Matched Filtering

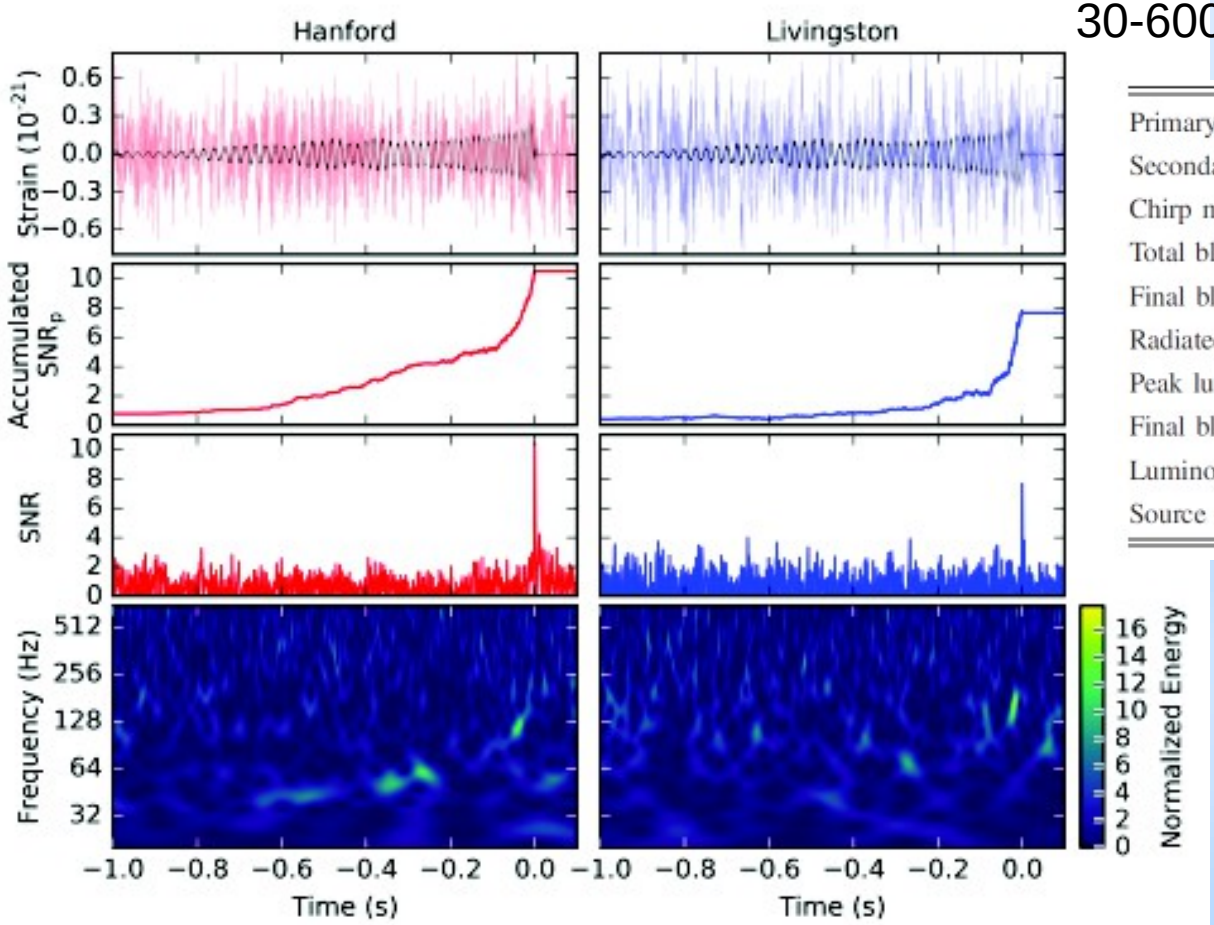

30-600 Hz bandpass

Primary black hole mass	$14.2^{+8.3}_{-3.7} M_\odot$
Secondary black hole mass	$7.5^{+2.3}_{-2.3} M_\odot$
Chirp mass	$8.9^{+0.3}_{-0.3} M_\odot$
Total black hole mass	$21.8^{+5.9}_{-1.7} M_\odot$
Final black hole mass	$20.8^{+6.1}_{-1.7} M_\odot$
Radiated gravitational-wave energy	$1.0^{+0.1}_{-0.2} M_\odot c^2$
Peak luminosity	$3.3^{+0.8}_{-1.6} \times 10^{56}$ erg/s
Final black hole spin	$0.74^{+0.06}_{-0.06}$
Luminosity distance	440^{+180}_{-190} Mpc
Source redshift z	$0.09^{+0.03}_{-0.04}$

GW151226 – A Success For Matched Filtering

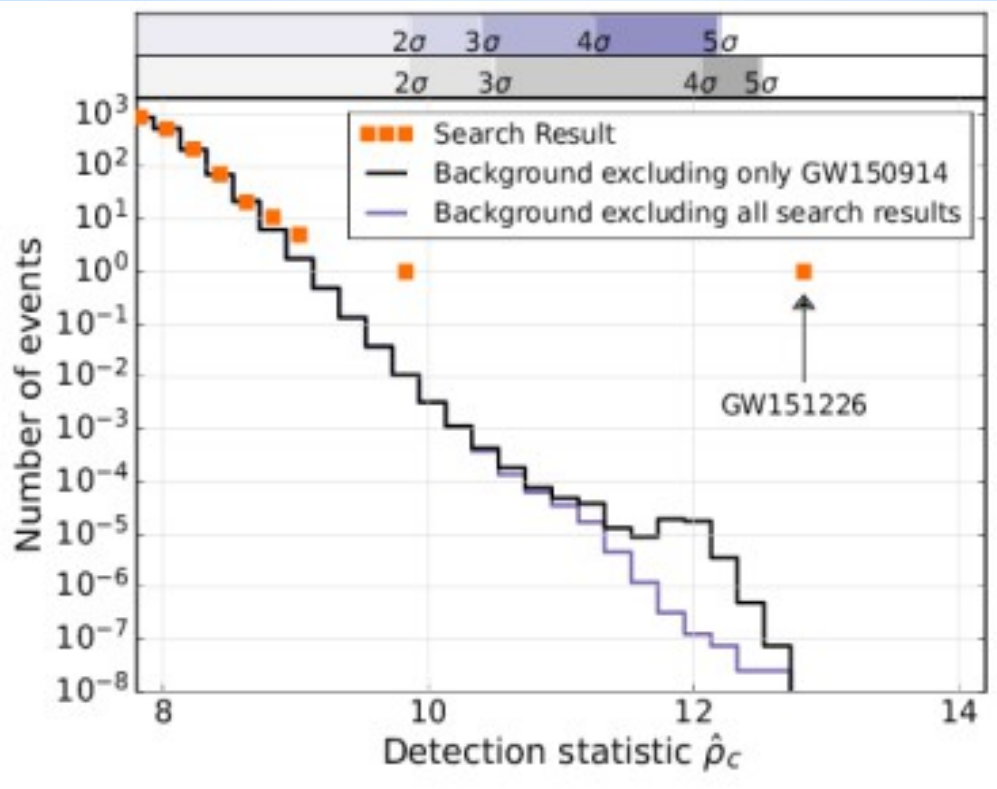

Results from our search for gravitational wave sources similar to GW151226 (and the previous detection GW150914) showing the significance of this detection compared to a background of false 'events' caused by noise from the LIGO instruments. We see that GW151226 is detected well above the level of the background.

Parameter Estimation

Presented here is a brief review the Bayesian approach to parameter estimation. The antenna output data is $\mathbf{z}(\mathbf{t})$, with joint probability distribution function (PDF) denoted by $p(\mathbf{z}|\boldsymbol{\theta})$ conditional on unobserved parameters $\boldsymbol{\theta} = (\theta_1, \ldots, \theta_d)$. The PDF $p(\mathbf{z}|\boldsymbol{\theta})$ is usually referred to as the *likelihood* and regarded as a function of the parameters $\boldsymbol{\theta}$. A Bayesian approach treats $\boldsymbol{\theta}$ as a random variable with a probability distribution that reflects the researcher's uncertainty about the parameters. Bayesian inference requires the specification of a *prior* PDF for $\boldsymbol{\theta}$, $p(\boldsymbol{\theta})$, that contains all prior information about $\boldsymbol{\theta}$. Information about $\boldsymbol{\theta}$ from the experiment is contained in the likelihood. Bayesian inference tells how the data $\mathbf{z}$ changes the knowledge about $\boldsymbol{\theta}$. From Bayes' theorem, this post-experimental knowledge about $\boldsymbol{\theta}$ is expressed through the *posterior* PDF

$$p(\boldsymbol{\theta}|\mathbf{z}) = \frac{p(\boldsymbol{\theta})p(\mathbf{z}|\boldsymbol{\theta})}{m(\mathbf{z})} \propto p(\boldsymbol{\theta})p(\mathbf{z}|\boldsymbol{\theta}) \tag{1}$$

where $m(\mathbf{z}) = \int p(\mathbf{z}|\boldsymbol{\theta})p(\boldsymbol{\theta})d\boldsymbol{\theta}$ is the marginal PDF of $\mathbf{z}$ which can be regarded as a normalizing constant as it is independent of $\boldsymbol{\theta}$. The posterior PDF is thus proportional to the product of prior and likelihood.

The standard Bayesian point estimate of a single parameter, say θ_i, is the posterior mean

$$\hat{\theta}_i = \int \theta_i p(\theta_i|\mathbf{z})d\theta_i \tag{2}$$

where

$$p(\theta_i|\mathbf{z}) = \int \ldots \int p(\boldsymbol{\theta}|\mathbf{z})d\theta_1 \ldots d\theta_{i-1}d\theta_{i+1} \ldots d\theta_d. \tag{3}$$

is the marginal posterior PDF. A measure of the uncertainty of this estimate is the posterior standard

Markov Chain Monte Carlo

and then accepted or rejected with some probability. However, the candidate generating PDF, $q(\boldsymbol{\theta}|\boldsymbol{\theta}_n)$ can now depend on the current state $\boldsymbol{\theta}_n$ of the Markov chain. A new candidate $\boldsymbol{\theta}'$ is accepted with a certain *acceptance probability* $\alpha(\boldsymbol{\theta}'|\boldsymbol{\theta}_n)$ also depending on the current state $\boldsymbol{\theta}_n$ given by

$$\alpha(\boldsymbol{\theta}'|\boldsymbol{\theta}_n) = \min\left\{\frac{p(\boldsymbol{\theta}')p(\mathbf{z}|\boldsymbol{\theta}')q(\boldsymbol{\theta}_n|\boldsymbol{\theta}')}{p(\boldsymbol{\theta}_n)p(\mathbf{z}|\boldsymbol{\theta}_n)q(\boldsymbol{\theta}'|\boldsymbol{\theta}_n)}, 1\right\}$$

if $(p(\boldsymbol{\theta}_n)p(\mathbf{z}|\boldsymbol{\theta}_n)q(\boldsymbol{\theta}'|\boldsymbol{\theta}_n)) > 0$, and $\alpha(\boldsymbol{\theta}'|\boldsymbol{\theta}_n) = 1$ otherwise. For good efficiency a multivariate normal distribution is often used for $q(\boldsymbol{\theta}|\boldsymbol{\theta}_n)$.

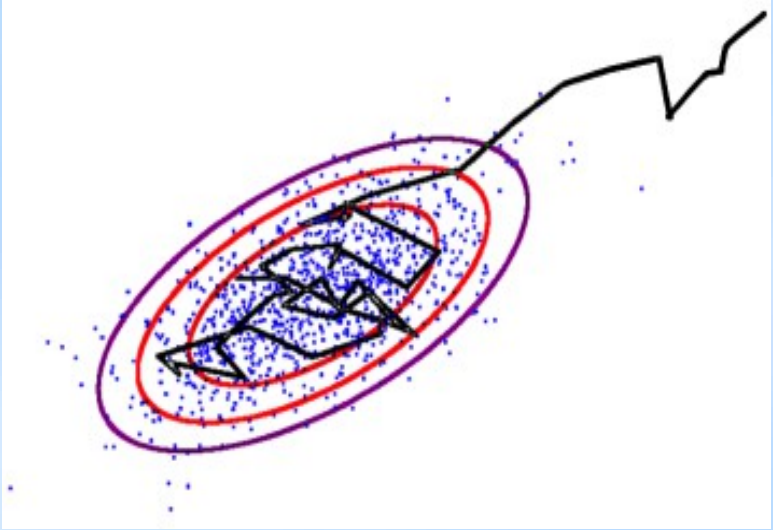

O1 Events

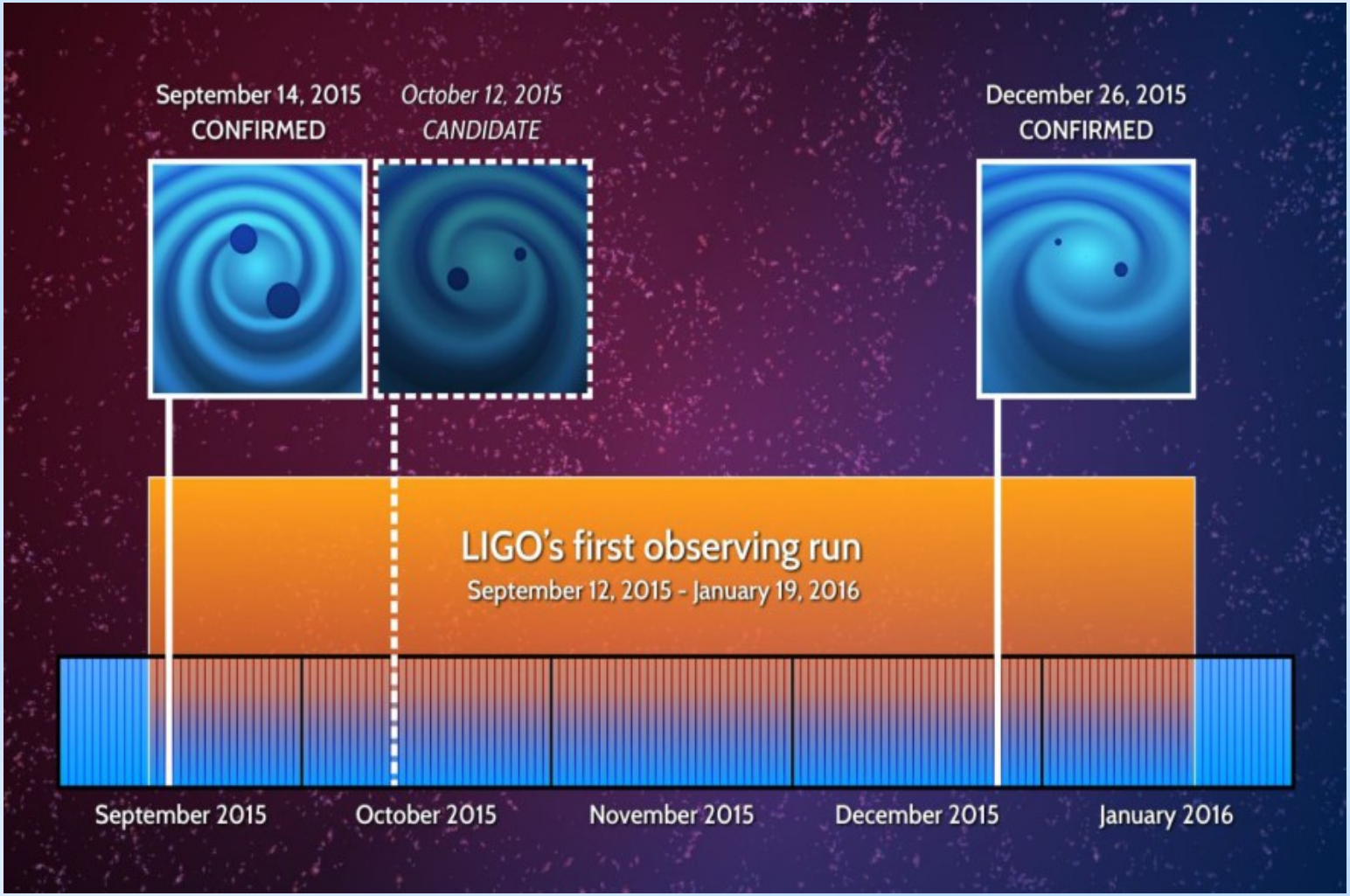

Image Credit - LIGO

Observing Run O2

30 November 2016 to 25 August 2017

Advanced Virgo 1 August – 25 August 2017

GW170814 – 3 Detector Observation

GW170814 : A three-detector observation of gravitational waves from a binary black hole coalescence

The LIGO Scientific Collaboration and The Virgo Collaboration

On August 14, 2017 at 10:30:43 UTC, the Advanced Virgo detector and the two Advanced LIGO detectors coherently observed a transient gravitational-wave signal produced by the coalescence of two stellar mass black holes, with a false-alarm-rate of $\lesssim 1$ in 27000 years. The signal was observed with a three-detector network matched-filter signal-to-noise ratio of 18. The inferred masses of the initial black holes are $30.5^{+5.7}_{-3.0}$ $M_\odot$ and $25.3^{+2.8}_{-4.2}$ $M_\odot$ (at the 90% credible level). The luminosity distance of the source is 540^{+130}_{-210} Mpc, corresponding to a redshift of $z = 0.11^{+0.03}_{-0.04}$. A network of three detectors improves the sky localization of the source, reducing the area of the 90% credible region from 1160 deg^2 using only the two LIGO detectors to 60 deg^2 using all three detectors. For the first time, we can test the nature of gravitational wave polarizations from the antenna response of the LIGO-Virgo network, thus enabling a new class of phenomenological tests of gravity.

Virgo has arrived!

A real world-wide network of gravitational wave detectors.

PRL

GW170814 – 3 Detector Observation

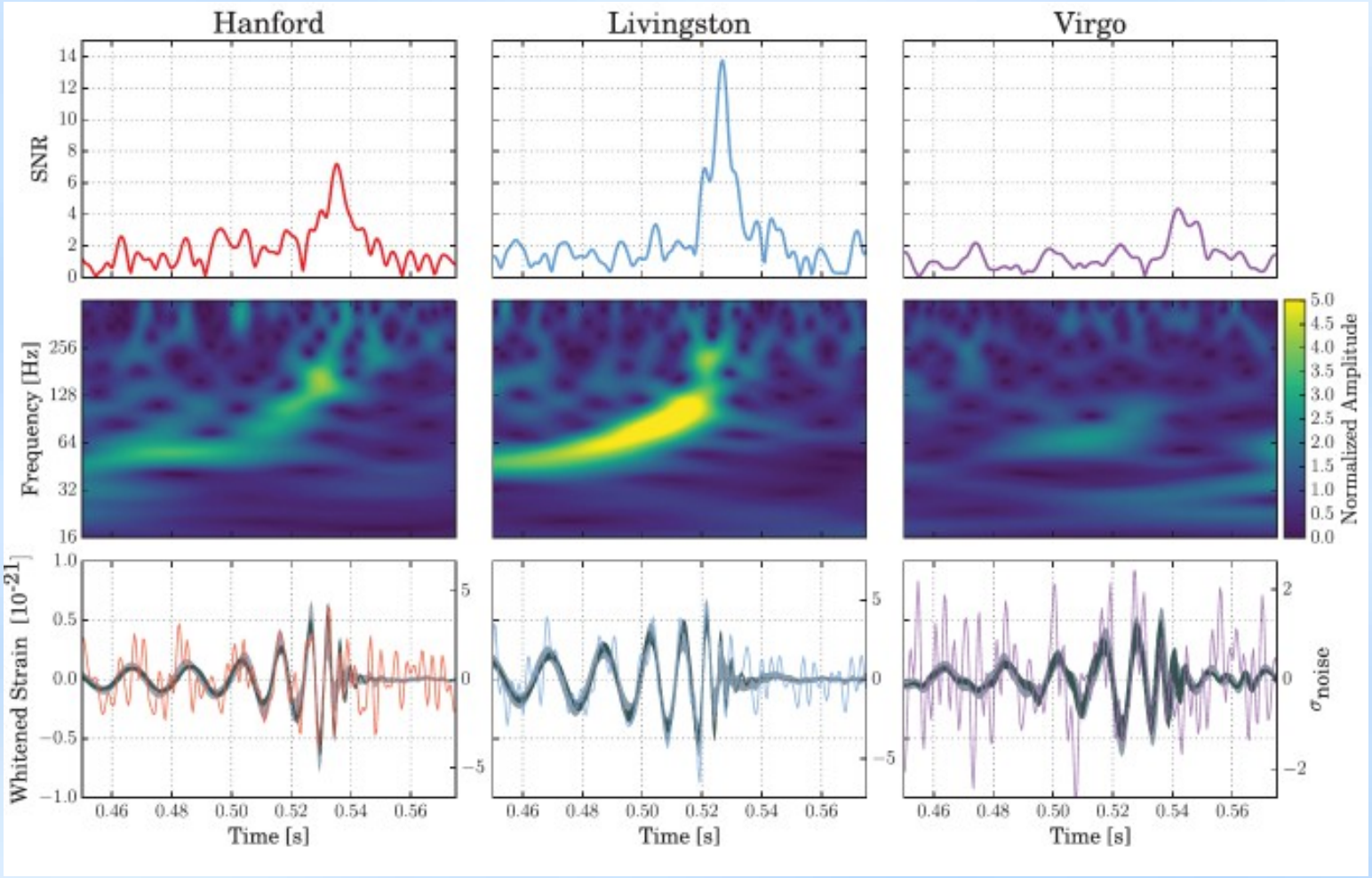

GW170814 – 3 Detector Observation

TABLE I: Source parameters for GW170814: median values with 90% credible intervals. We quote source-frame masses; to convert to the detector frame, multiply by $(1 + z)$ [120, 121]. The redshift assumes a flat cosmology with Hubble parameter $H_0 = 67.9\ \mathrm{km\,s^{-1}\,Mpc^{-1}}$ and matter density parameter $\Omega_\mathrm{m} = 0.3065$ [122].

Primary black hole mass m_1	$30.5^{+5.7}_{-3.0}\ \mathrm{M_\odot}$
Secondary black hole mass m_2	$25.3^{+2.8}_{-4.2}\ \mathrm{M_\odot}$
Chirp mass $\mathcal{M}$	$24.1^{+1.4}_{-1.1}\ \mathrm{M_\odot}$
Total mass M	$55.9^{+3.4}_{-2.7}\ \mathrm{M_\odot}$
Final black hole mass M_f	$53.2^{+3.2}_{-2.5}\ \mathrm{M_\odot}$
Radiated energy E_rad	$2.7^{+0.4}_{-0.3}\ \mathrm{M_\odot c^2}$
Peak luminosity ℓ_peak	$3.7^{+0.5}_{-0.5} \times 10^{56}\ \mathrm{erg\,s^{-1}}$
Effective inspiral spin parameter χ_eff	$0.06^{+0.12}_{-0.12}$
Final black hole spin a_f	$0.70^{+0.07}_{-0.05}$
Luminosity distance D_L	$540^{+130}_{-210}\ \mathrm{Mpc}$
Source redshift z	$0.11^{+0.03}_{-0.04}$

GW170814 – 3 Detector Observation

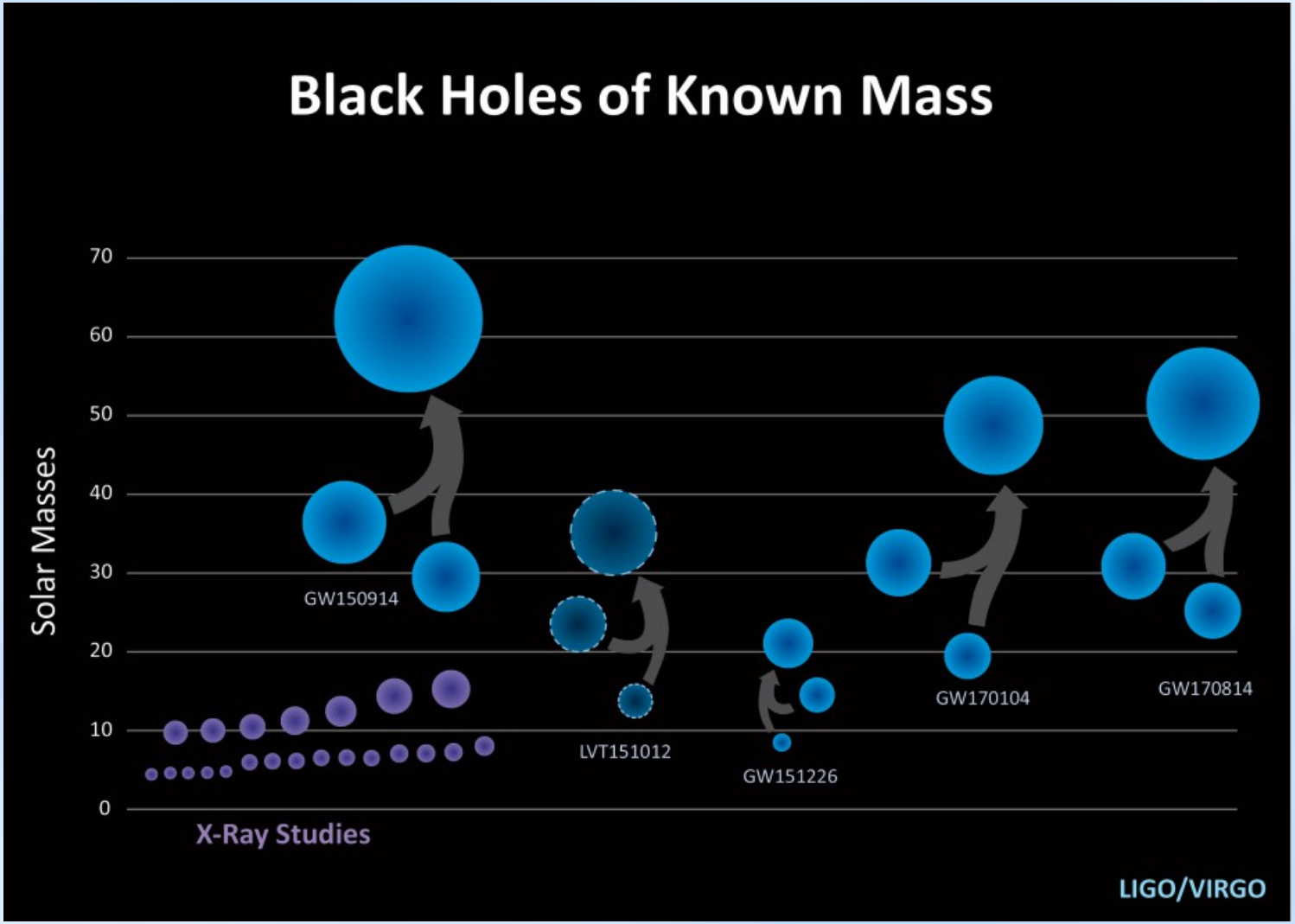

Population of Black Holes

LIGO/Caltech/Sonoma State (Aurore Simonnet)]

GW170814 – 3 Detector Observation

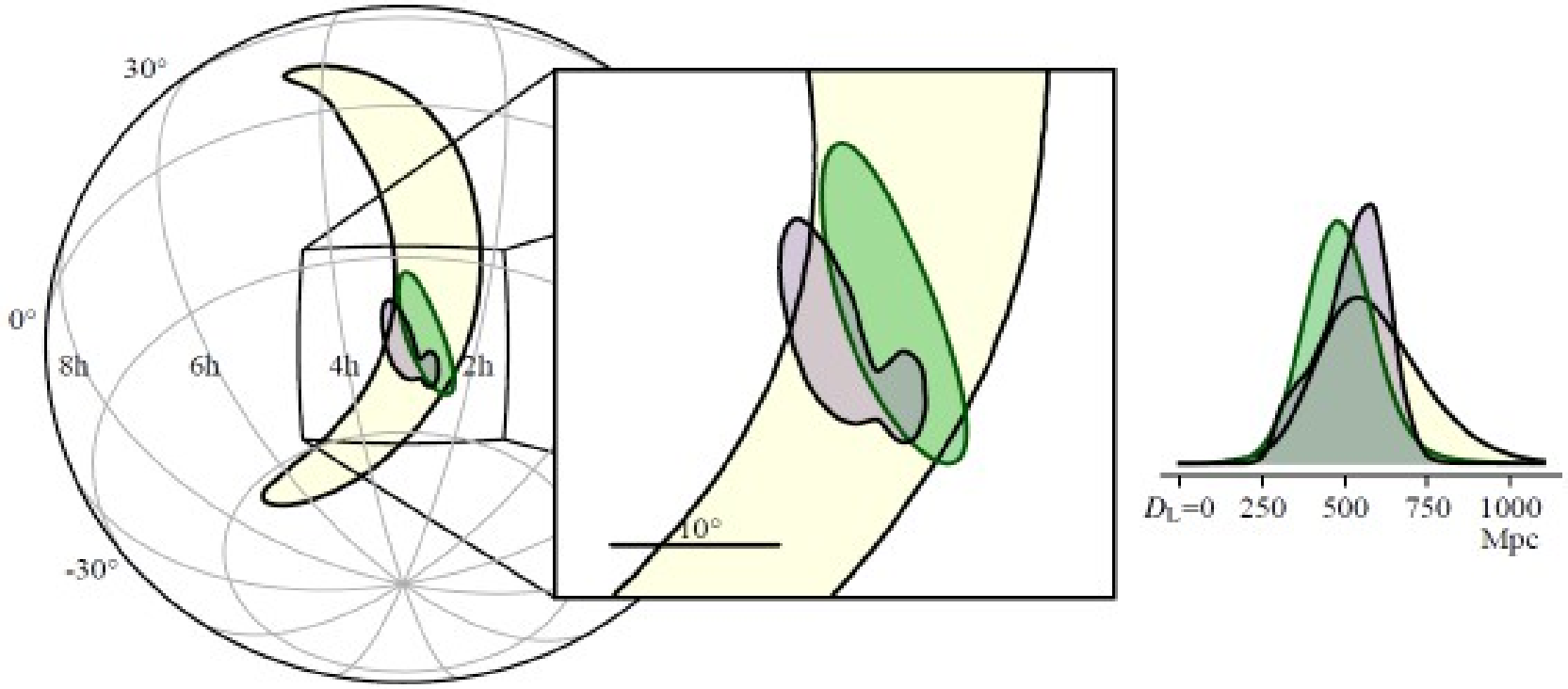

FIG. 3: Localization of GW170814. The rapid localization using data from the two LIGO sites is shown in yellow, with the inclusion of data from Virgo shown in green. The full Bayesian localization is shown in purple. The contours represent the 90% credible regions. The left panel is an orthographic projection and the inset in the center is a gnomonic projection; both are in equatorial coordinates. The inset on the right shows the posterior probability distribution for the luminosity distance, marginalized over the whole sky.

1160 sq. deg 2 LIGOs only →
60 sq. deg for 2 LIGOs + Virgo

Sky Position Estimation Comparison

Skymap of the LIGO/Virgo black hole mergers. This three-dimensional projection of the Milky Way galaxy onto a transparent globe shows the probable locations of the black hole mergers.

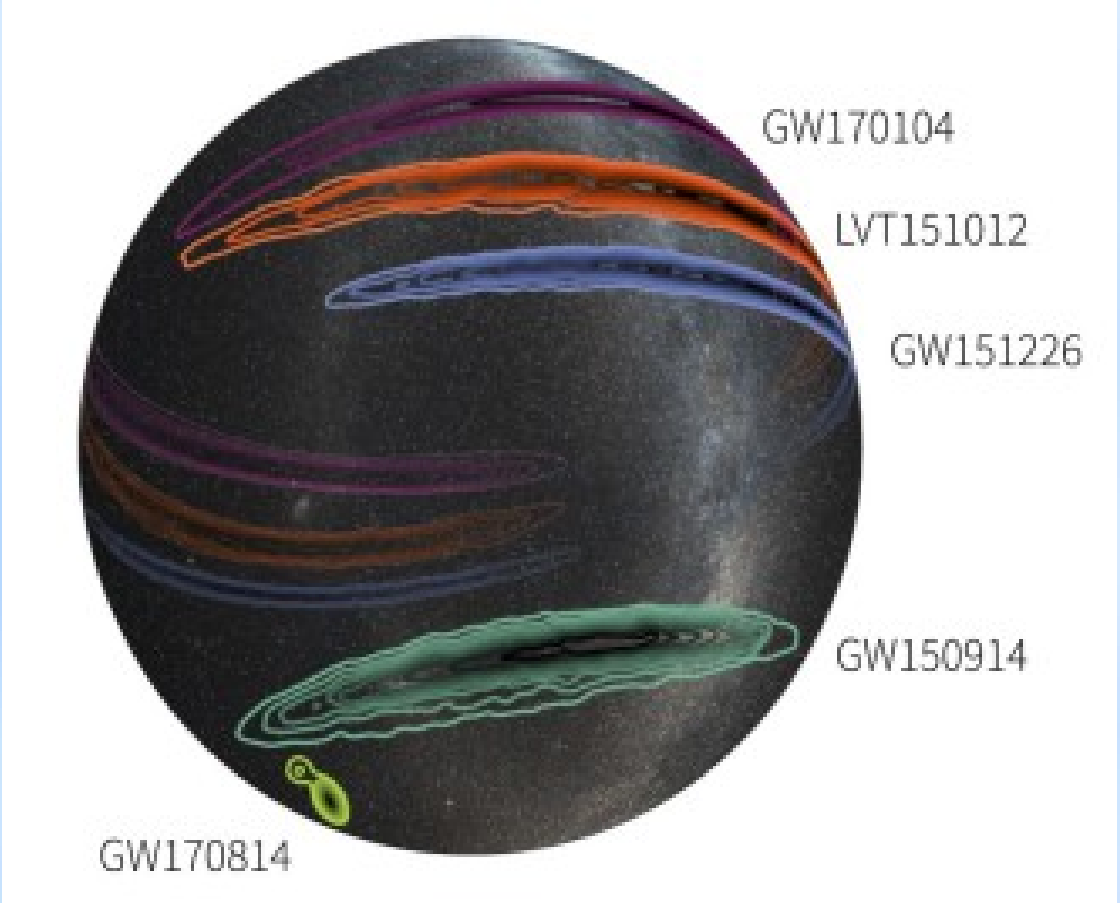

LIGO/Virgo/Caltech/MIT/Leo Singer (Milky Way image: Axel Mellinger

Observed Gravitational Wave Signals

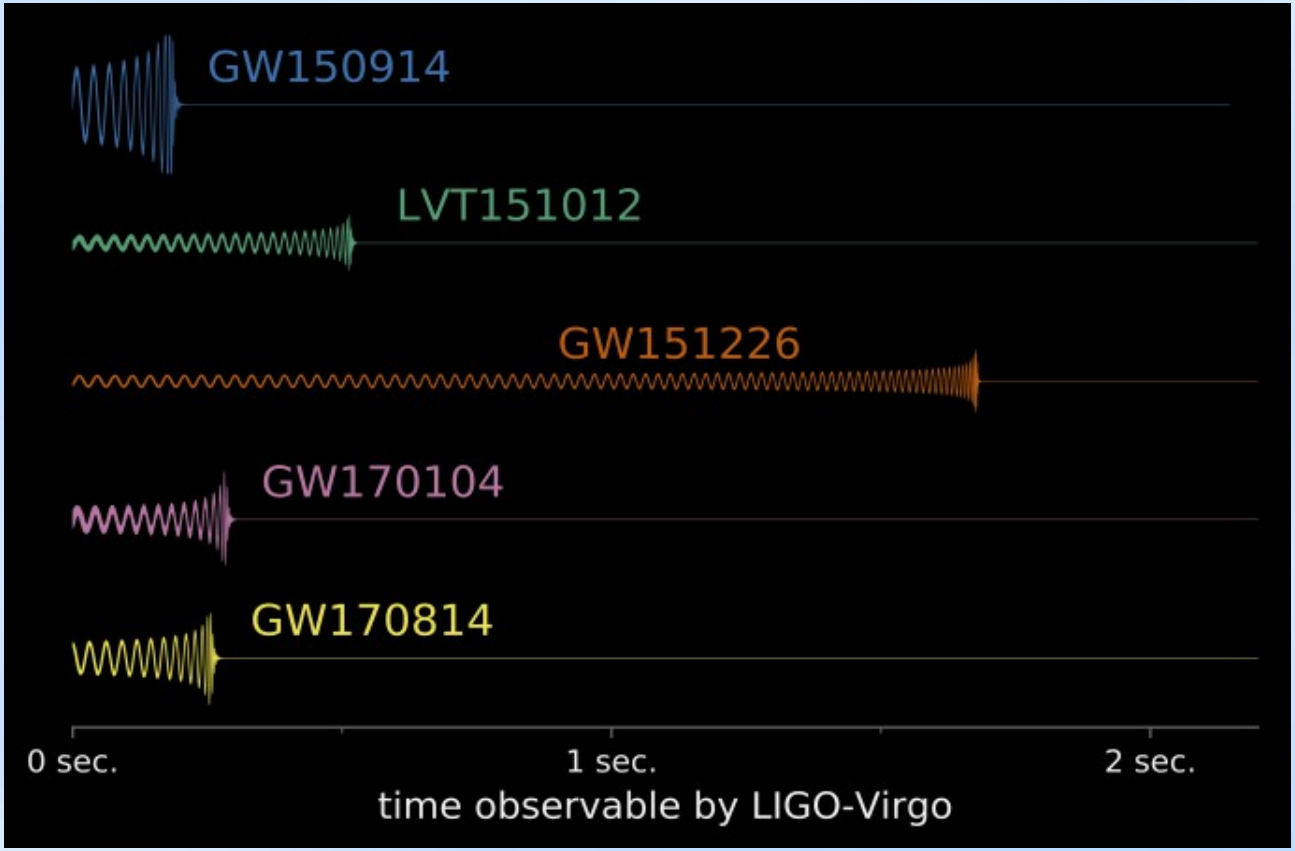

LIGO/Virgo/B. Farr (University of Oregon)]

Testing General Relativity With GW170814

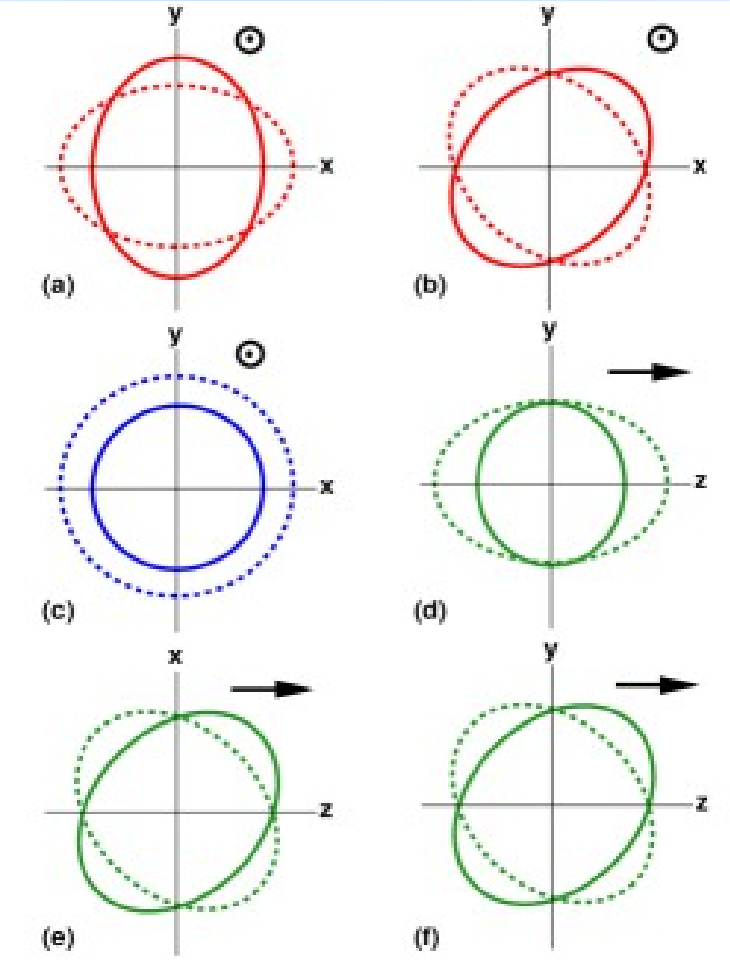

We now have a network of detectors with different orientations (2 LIGO are almost co-aligned, Virgo is not).

Allows the study of polarization of the gravitational waves.

Results favor purely tensor polarization against purely vector and purely scalar.

Tests of GR performed similar to those carried out for the previous confirmed detections — similar results, consistent with the predictions of Einstein's theory.

Post-Newtonian tests, signal consistency, ...

Clifford Will, Living Reviews in Relativity)

Testing General Relativity

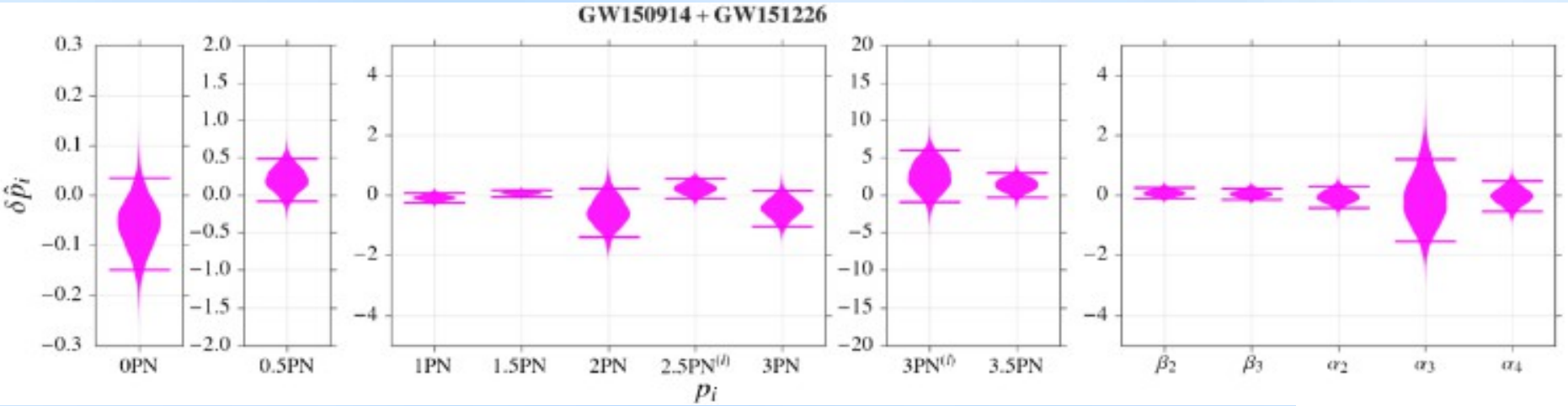

PHYS. REV. X 6, 041015 (2016)

Posterior density distributions for relative deviations in the PN, intermediate, and merger-ringdown parameters.

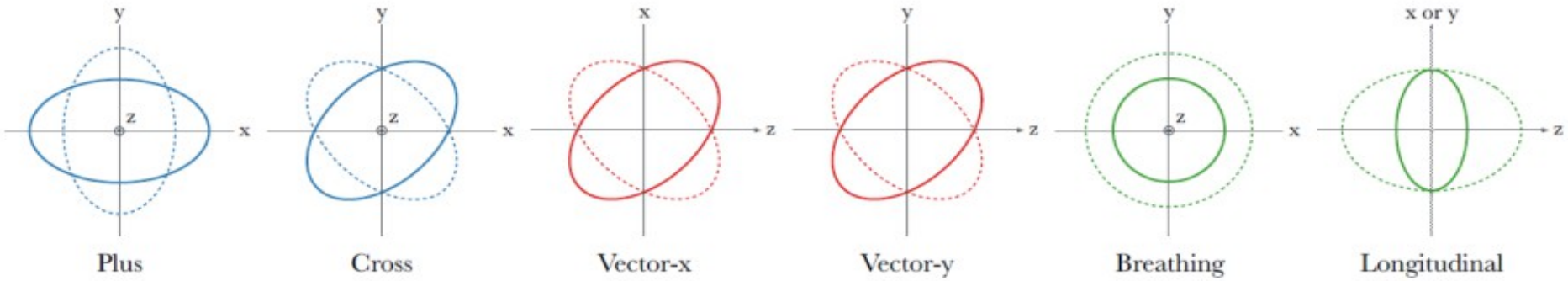

arXiv:1704.08373

arXiv:1709.09203

Modified Gravity Theories : Searches including extra polarizations (Stochastic and CW)

Astrophysics: Binary Black Hole Formation

- Isolated Binaries
  - Solar to Population III
  - Rapid rotation

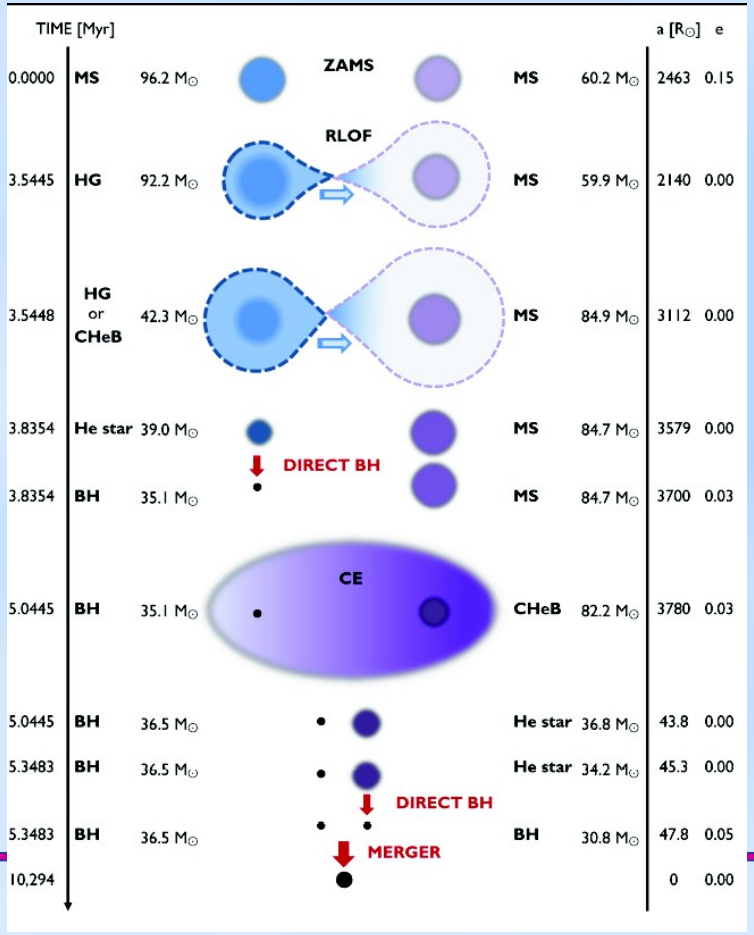

Belczynski et al.

- Dense Clusters
  - Globular clusters
  - Young clusters
  - Galactic centers

Low metallicity environment needed for large stellar mass black hole formation

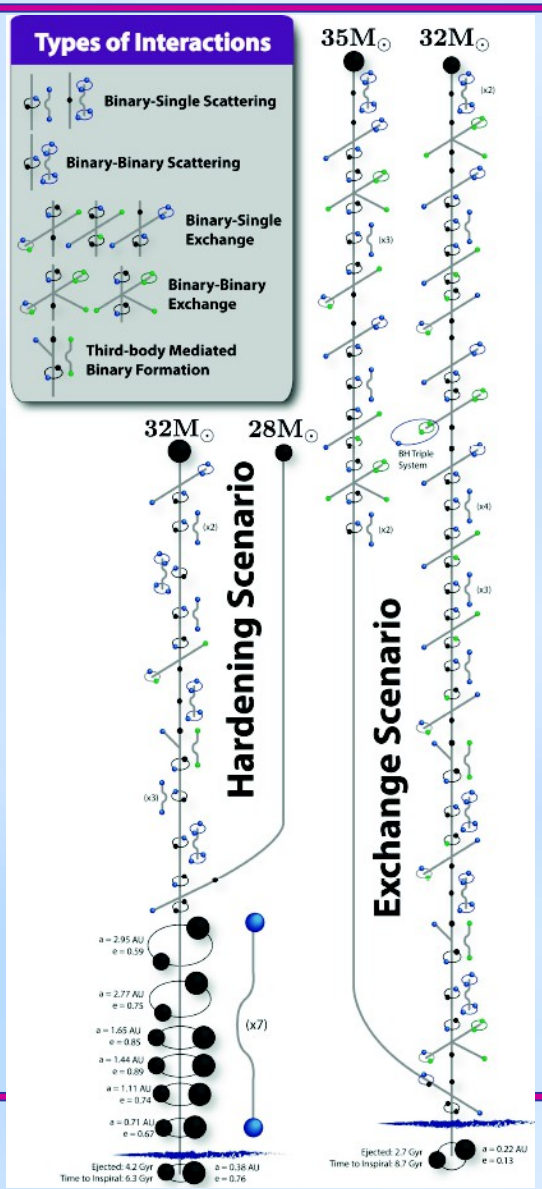

Arxiv 1602:02444, 1604:04254

Spin Observations Are Becoming Interesting

GW150914

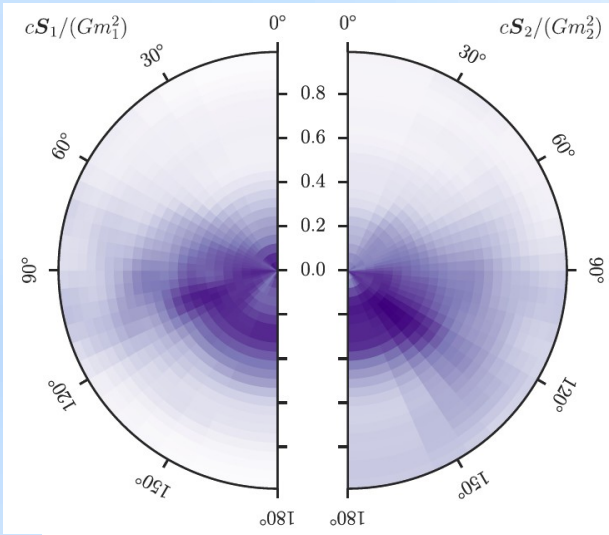

LVT151012

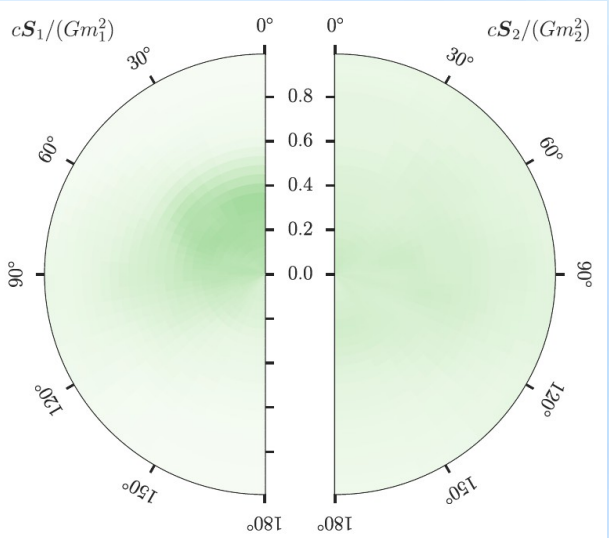

GW151226

No significant spin for GW170814

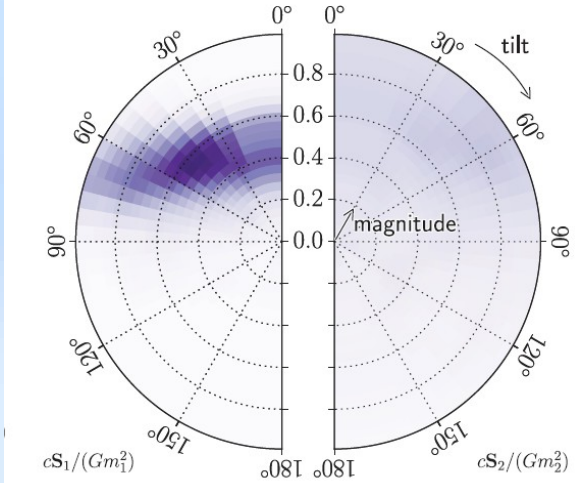

GW170114

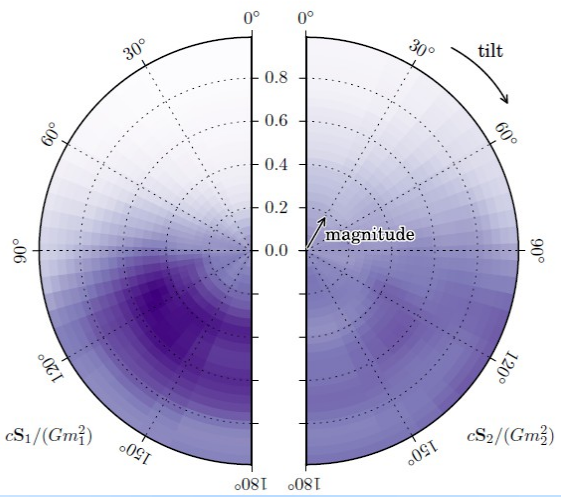

Isolated Binary Formation?

Cluster Formation?

GW170817 – The Birth of Multi-Messenger Astronomy

17 August 2017, 12:41…

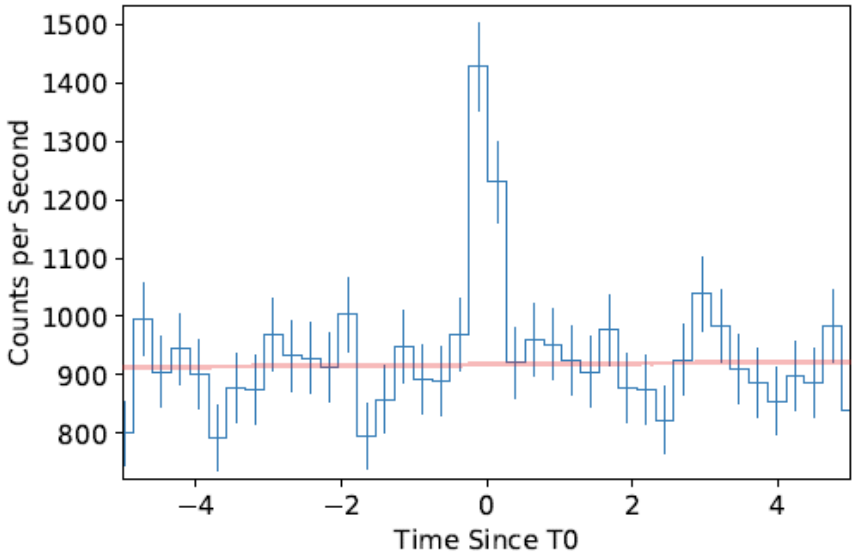


```
//////////////////////////////////////////////////////////////////////
TITLE:           GCN/FERMI NOTICE NOTICE_DATE:     Thu 17 Aug 17 12:41:20 UT
NOTICE_TYPE:     Fermi-GBM Alert RECORD_NUM:      1
TRIGGER_NUM:     524666471
GRB_DATE:        17982 TJD;   229 DOY;   17/08/17
GRB_TIME:        45666.47 SOD {12:41:06.47} UT
TRIGGER_SIGNIF:  4.8 [sigma]
TRIGGER_DUR:     0.256 [sec]
E_RANGE:         3-4 [chan]   47-291 [keV]
...
COMMENTS:        Fermi-GBM Trigger Alert.
COMMENTS:        This trigger occurred at longitude,latitude = 321.53,3.90 [deg].   COMMENTS:
   The LC_URL file will not be created until ~15 min after the trigger.
//////////////////////////////////////////////////////////////////////
```

GW170817 – LIGO and Virgo

- LIGO and Virgo were operational
- 12:47 (UTC): Automatic alert
- Signal consistent with binary neutron star merger
- Strong signal in LIGO Hanford
- Merger 1.7 s before Fermi GBM trigger
- Noise event “glitch” in LIGO Livingston, but the inspiral is visible before and after
- Data transfer problem from Virgo
- 13:21 first LIGO-Virgo alert issued

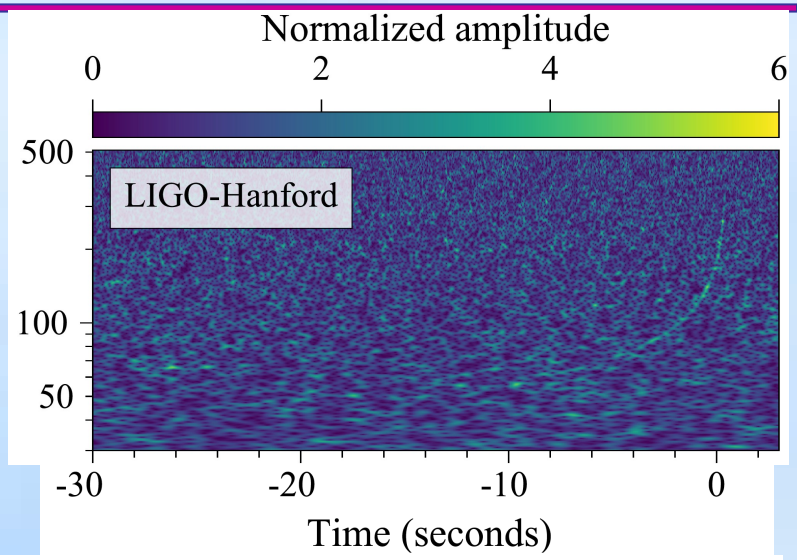

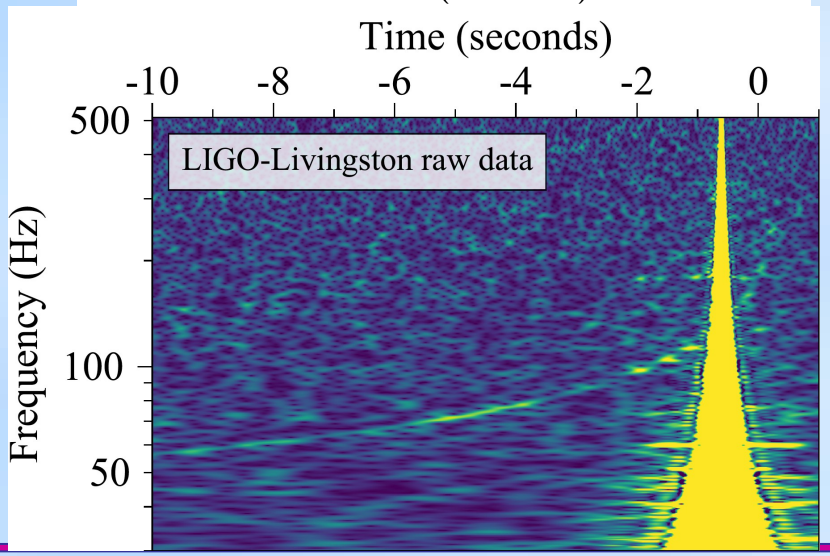

GRB 170817A and GW170817

- 6 minutes later a single interferometer trigger was seen by LIGO
- The LVC reported GW170817 to LV-EM collaborators as a possible joint detection about 40 minutes after event time
- The first constrained skymap for this event was the initial GBM localization
- The combine LIGO/Virgo skymap agreed with the GBM location, and reduced the area to about 30 deg^2

- **Further work shows an association significance of 5.3σ**

$\Delta t = 1.74 +/- 0.05$

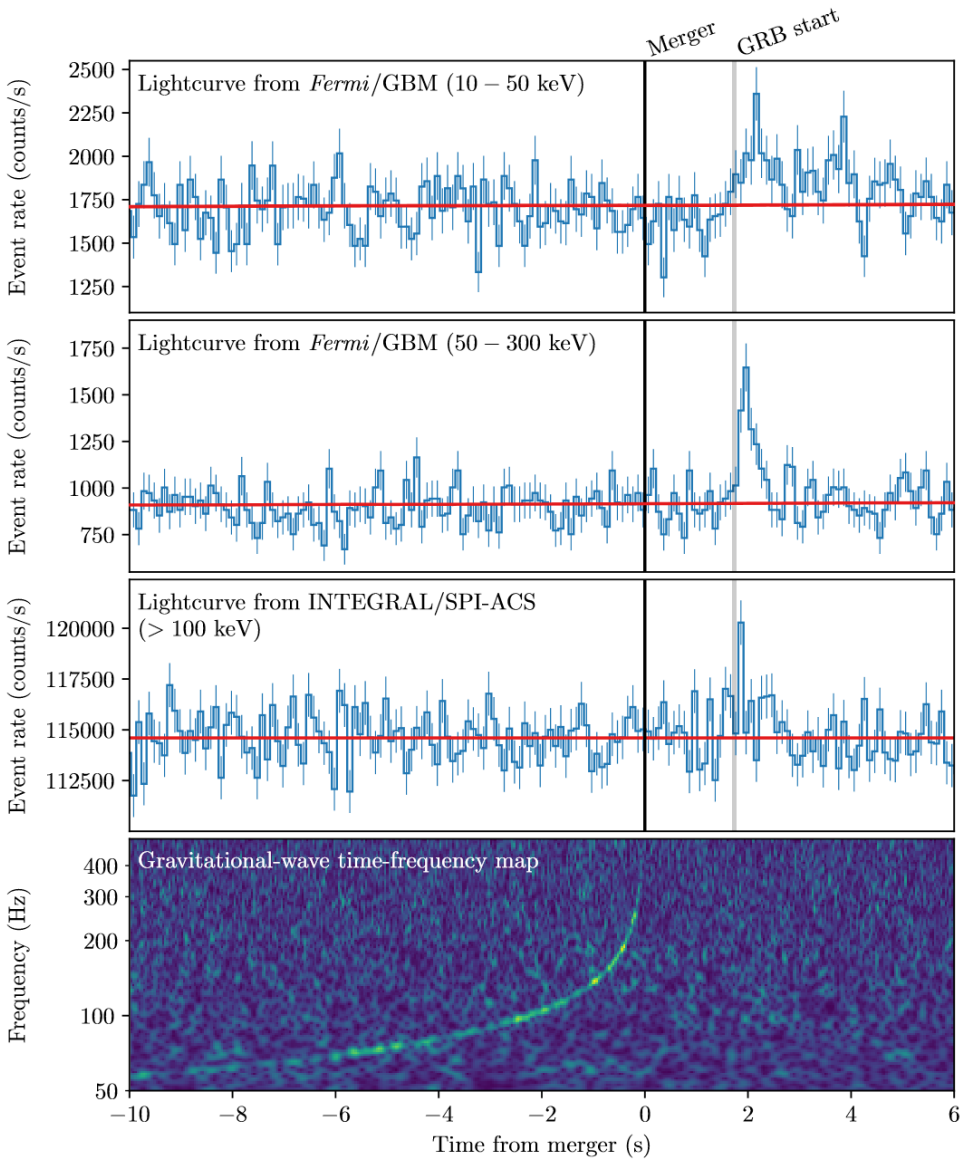

GW170817 – LIGO and Virgo

- Calculate the sky position of the source
- Contribution of Virgo is decisive
  - LIGO alone: 190 deg2
  - LIGO + Virgo
- LIGO-Virgo sky map much smaller than GRB (Fermi GBM + INTEGRAL)
- Gravitational waves give a distance: ~40 Mpc, ~140 million light years
- 17:54 the improved skymap is distributed to observing partners.
- Frantic preparations for observing at sunset in Chile

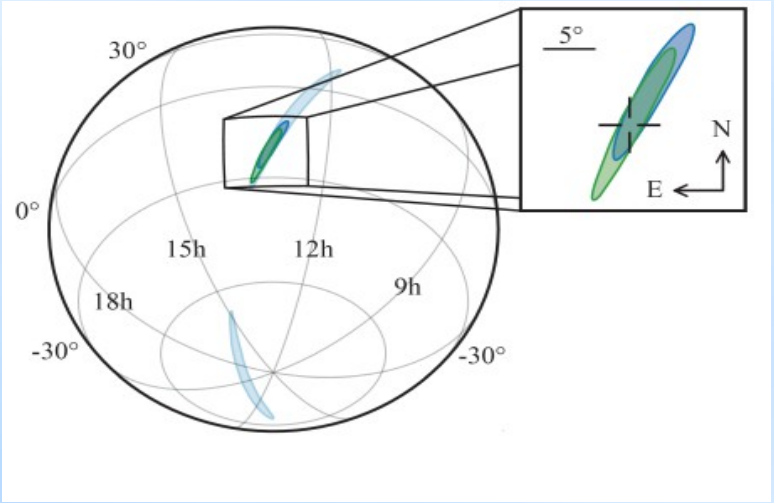

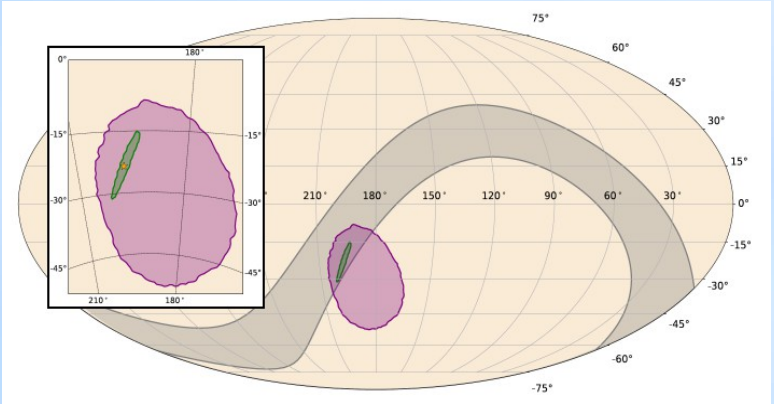

Optical search GW170817 source– Host Galaxy Found

T_0 + 12 hours :
Alert sent from 1m2H Swope

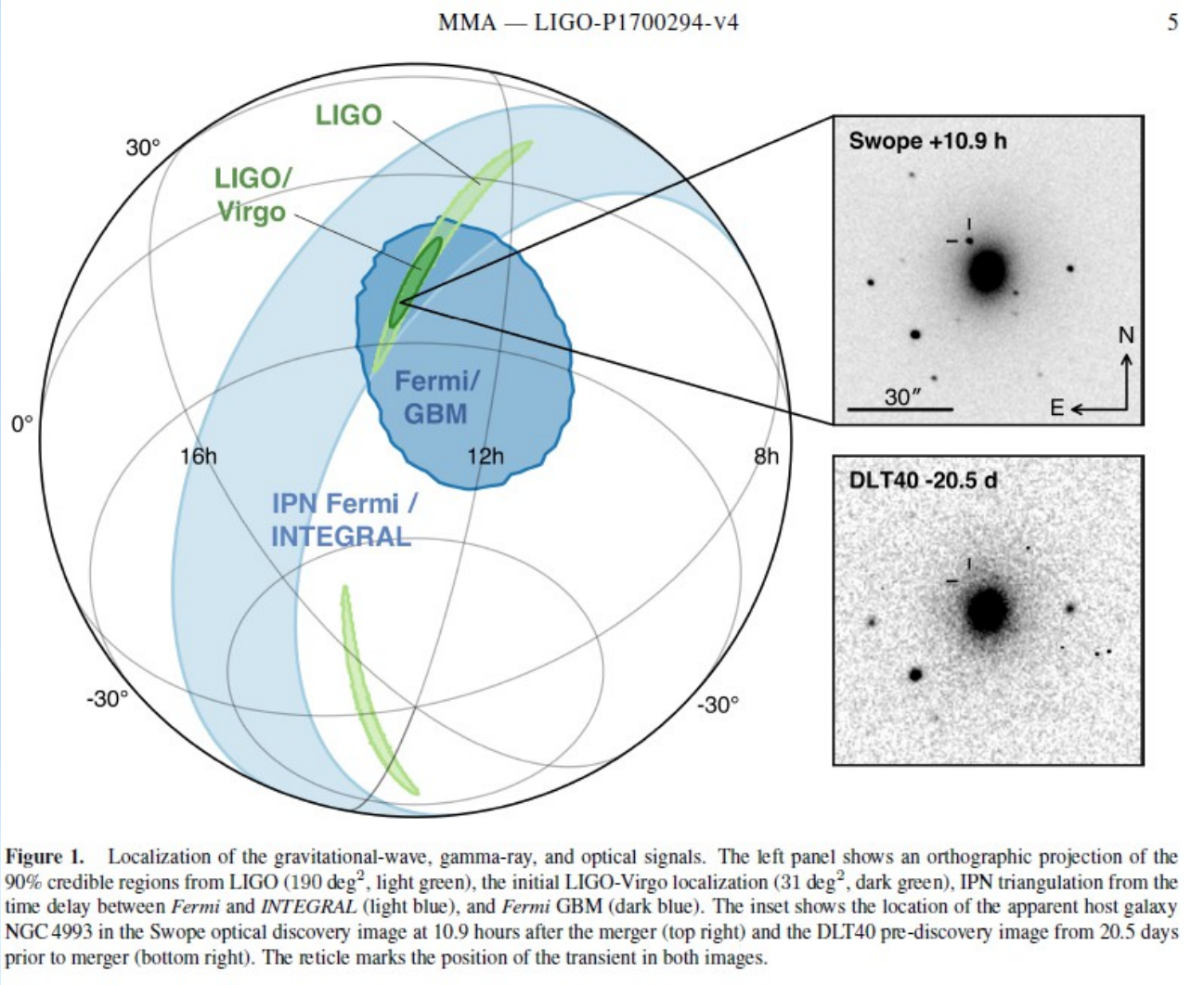

Figure 1. Localization of the gravitational-wave, gamma-ray, and optical signals. The left panel shows an orthographic projection of the 90% credible regions from LIGO (190 deg^2, light green), the initial LIGO-Virgo localization (31 deg^2, dark green), IPN triangulation from the time delay between *Fermi* and *INTEGRAL* (light blue), and *Fermi* GBM (dark blue). The inset shows the location of the apparent host galaxy NGC 4993 in the Swope optical discovery image at 10.9 hours after the merger (top right) and the DLT40 pre-discovery image from 20.5 days prior to merger (bottom right). The reticle marks the position of the transient in both images.

GW170817 – Host Galaxy Found

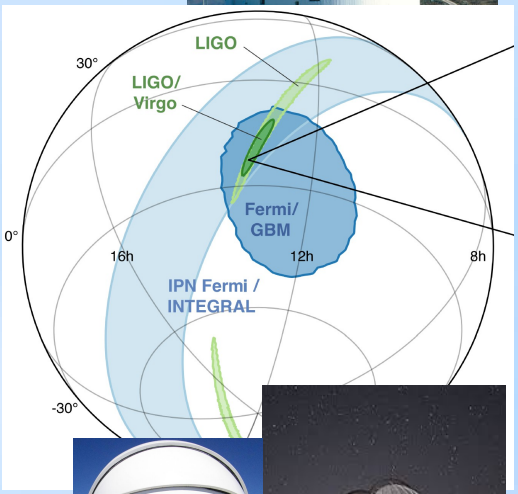

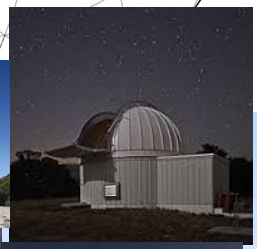

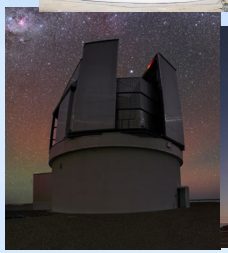

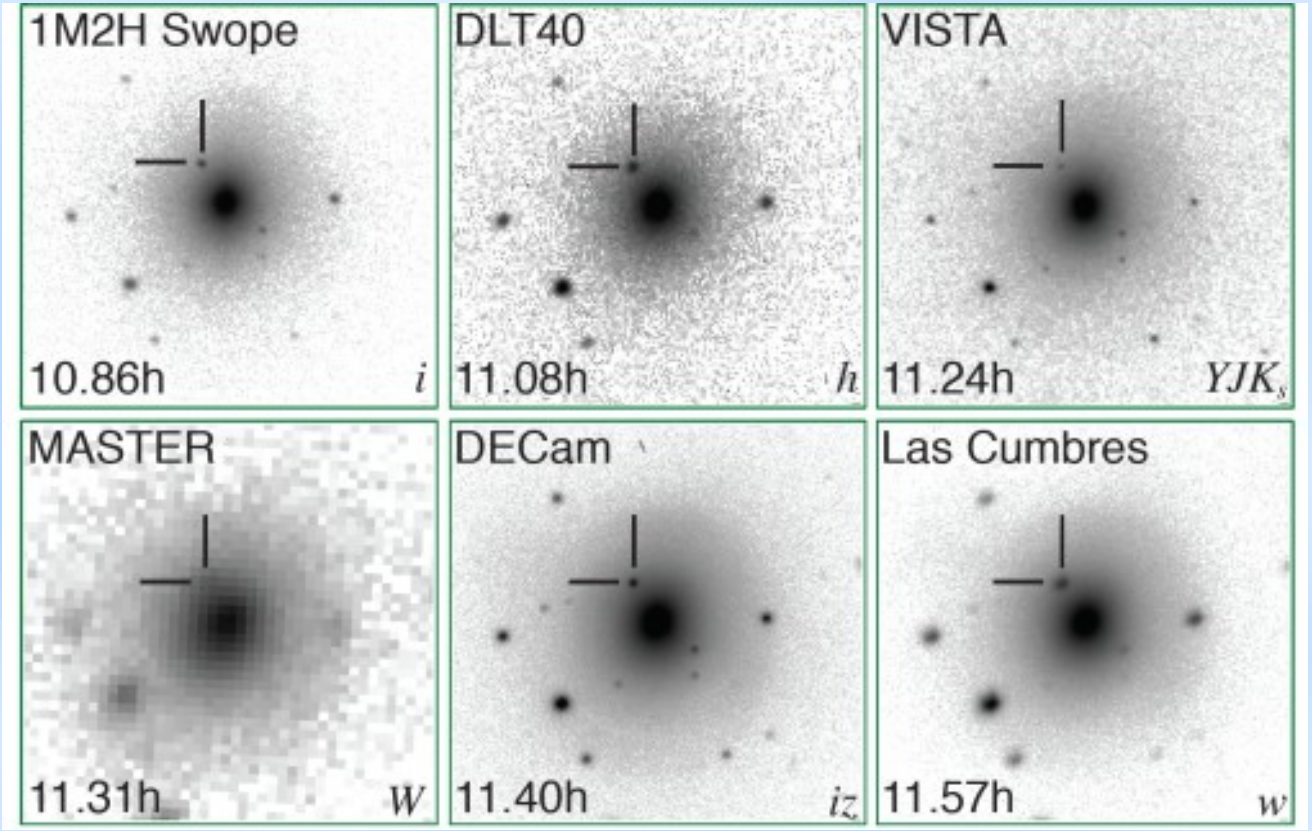

GW170817 – Host Galaxy Found

Host Galaxy: NGC 4993

Distance 42.9 +/- 3.2 Mpc
(140 +/- 10 Mly)

An Unprecedented Follow-up

70 observatories
192 “GCN” circulars
76 papers on arxiv on Tuesday.

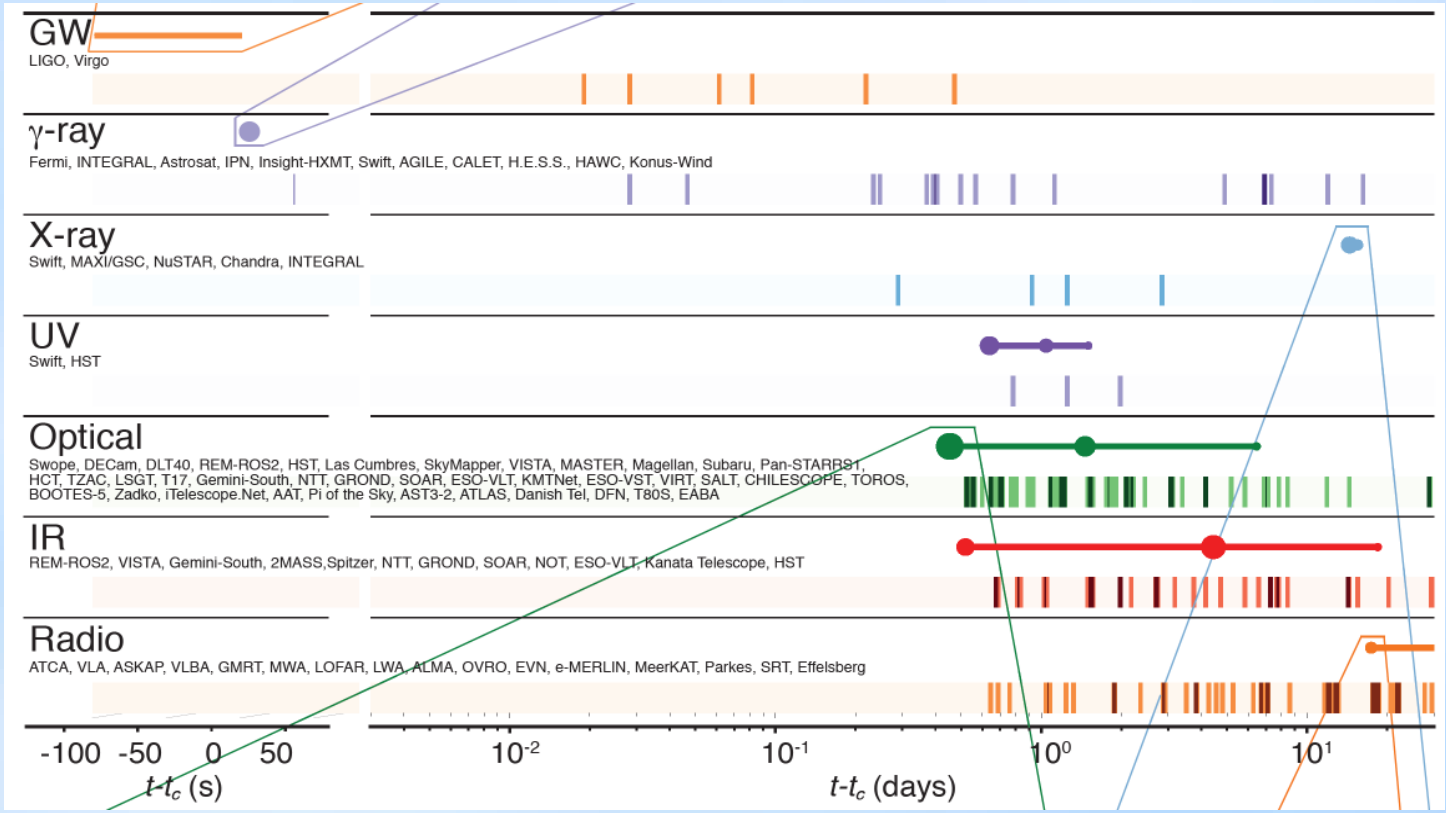

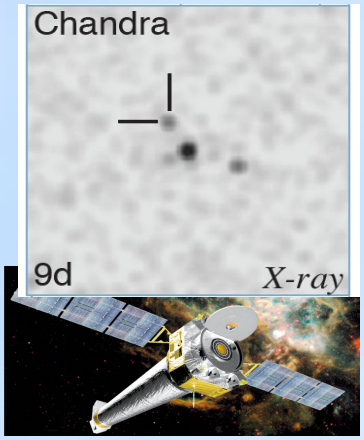

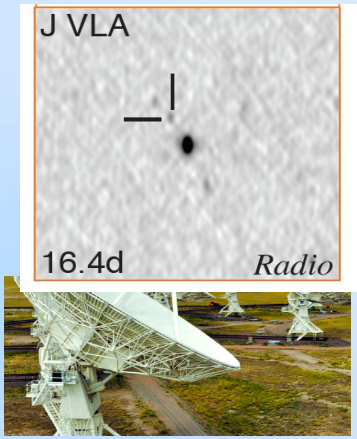

ApJ Lett

Kilonova

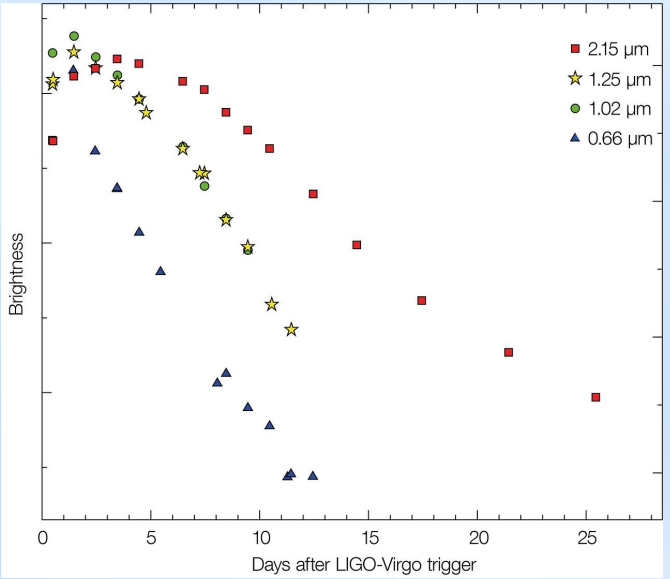

An initially blue signals that fades and turns to red.

All that glisters is not gold—
Often have you heard that told.

ApJ Lett

Kilonova

Ejected mass of 0.04 Mo

Velocity 0.2 c

Line feature for r-process with elements 90<A<140

“This indicates that neutron star mergers produce gravitational waves, radioactively powered kilonovae, and are a nucleosynthetic source of the r-process elements.”

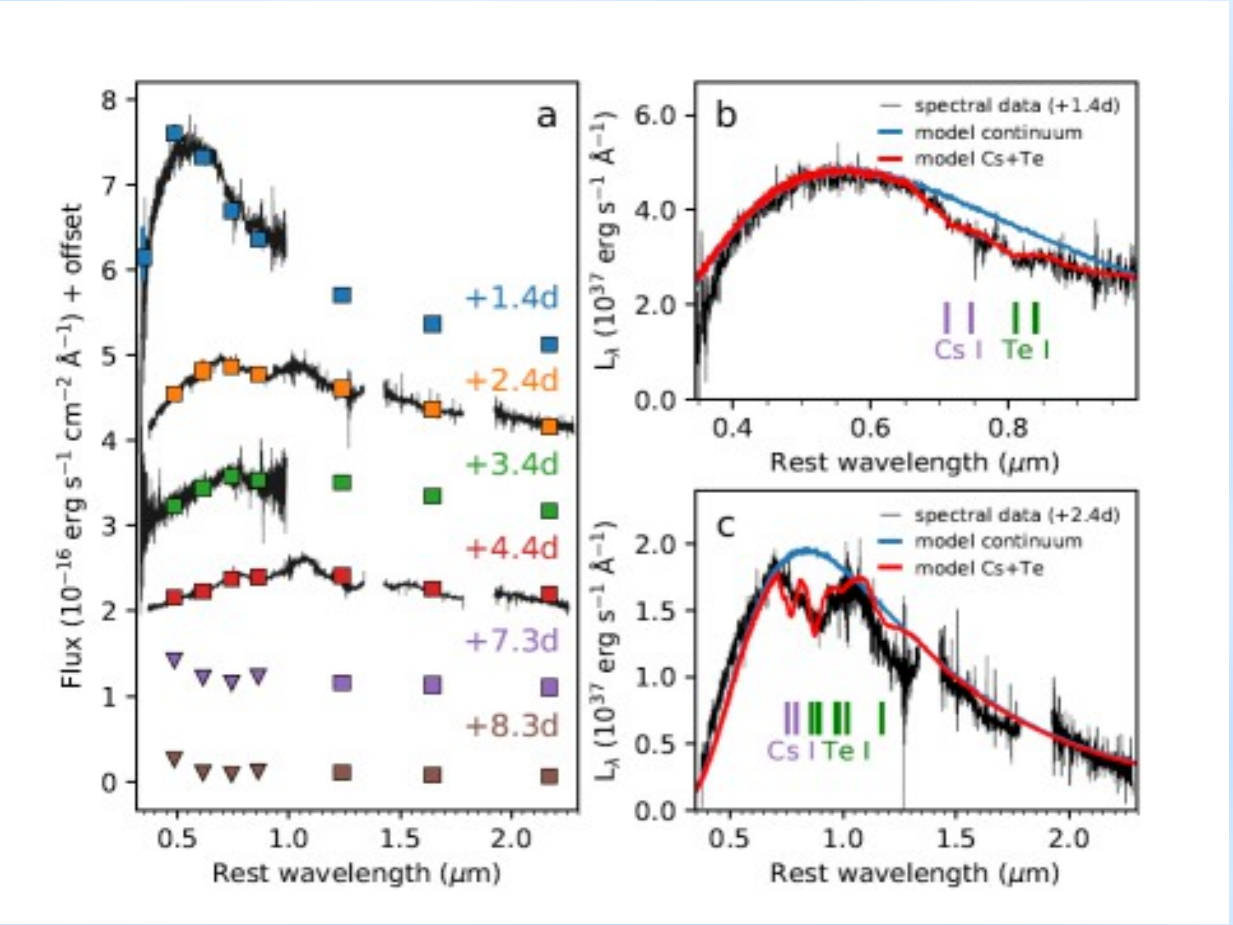

Pan-STARRSS. Smartt et al, Nature

A New Measurement of the Hubble Constant

We determine the Hubble constant to be $70.0^{+12.0}_{-8.0}\,\mathrm{km\,s^{-1}\,Mpc^{-1}}$

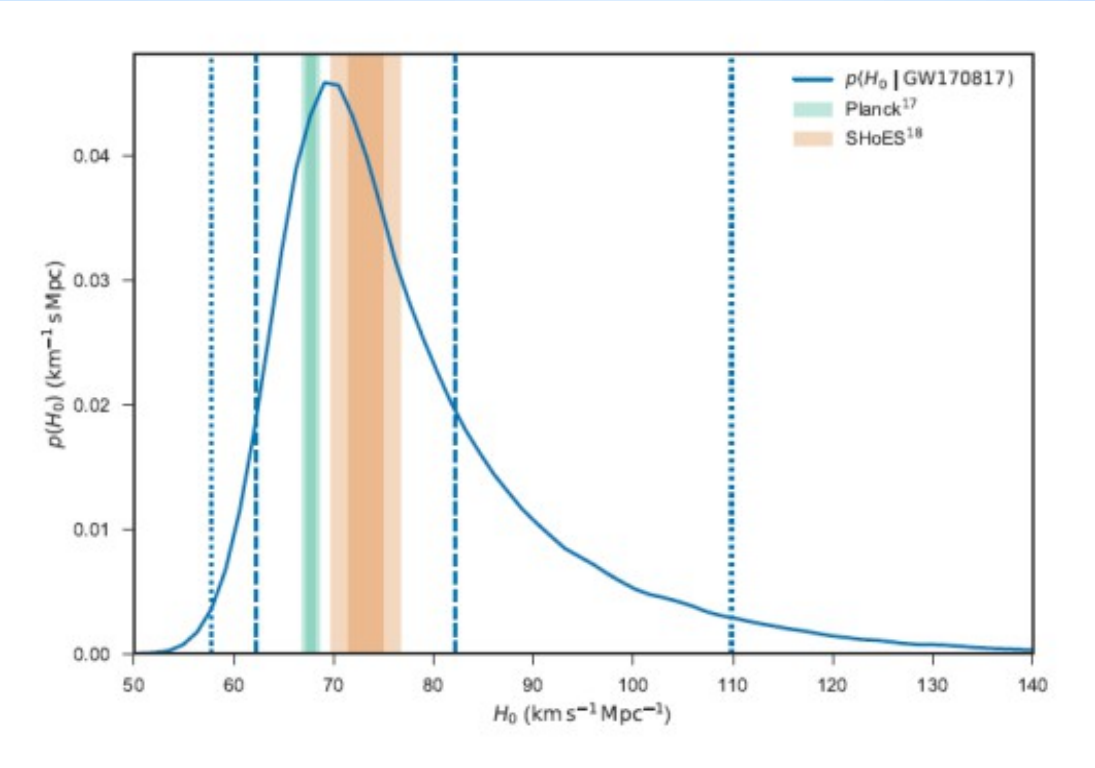

"Our measurement combines the distance to the source inferred purely from the gravitational-wave signal with the recession velocity inferred from measurements of the redshift using electromagnetic data."

Nature

A New Measurement of the Hubble Constant

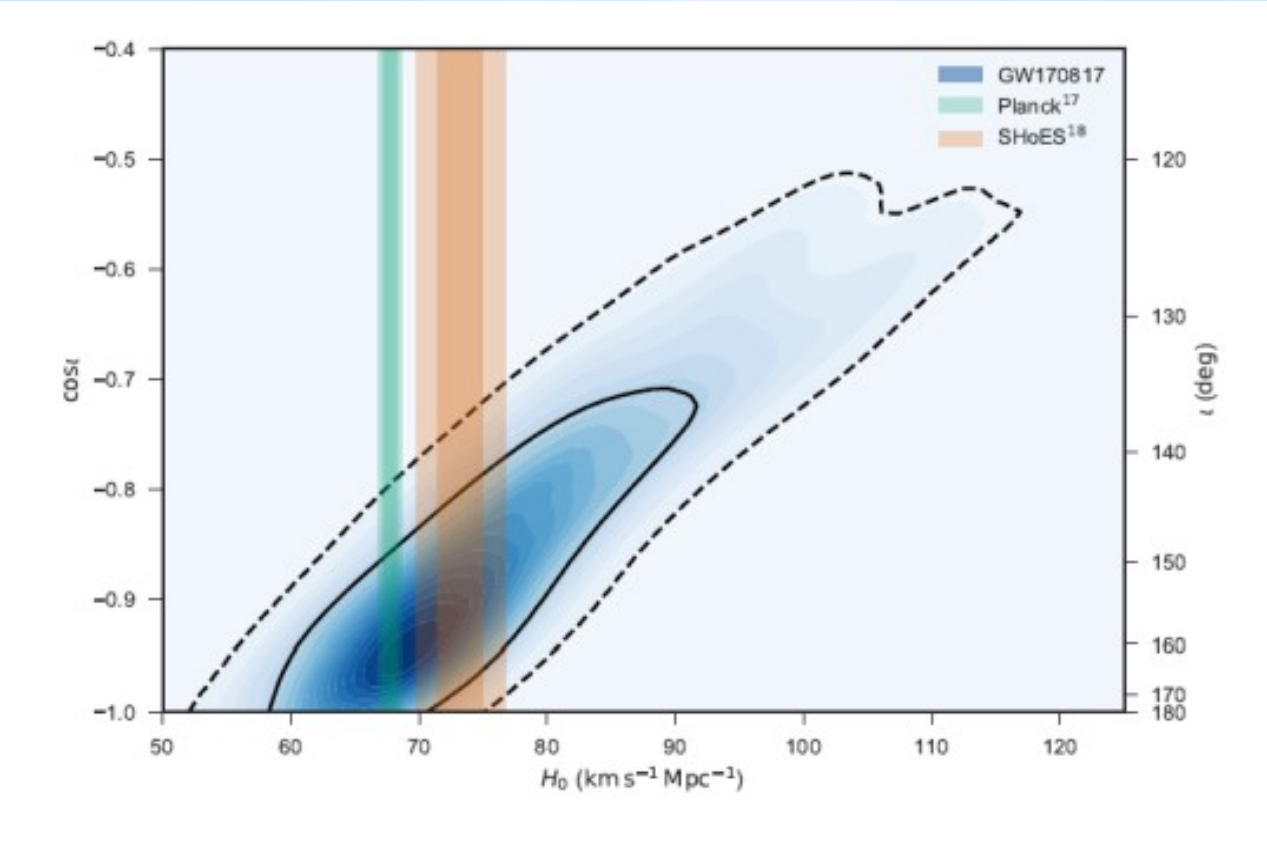

Inclination angles near 180 deg (cos i = -1) indicate that the orbital angular momentum is anti parallel with the direction from the source to the detector.

Binary System Parameters

TABLE I. Source properties for GW170817: we give ranges encompassing the 90% credible intervals for different assumptions of the waveform model to bound systematic uncertainty. The mass values are quoted in the frame of the source, accounting for uncertainty in the source redshift.

	Low-spin priors ($\|\chi\| \leq 0.05$)	High-spin priors ($\|\chi\| \leq 0.89$)
Primary mass m_1	1.36–1.60 $M_\odot$	1.36–2.26 $M_\odot$
Secondary mass m_2	1.17–1.36 $M_\odot$	0.86–1.36 $M_\odot$
Chirp mass $\mathcal{M}$	$1.188^{+0.004}_{-0.002} M_\odot$	$1.188^{+0.004}_{-0.002} M_\odot$
Mass ratio m_2/m_1	0.7–1.0	0.4–1.0
Total mass $m_{\rm tot}$	$2.74^{+0.04}_{-0.01} M_\odot$	$2.82^{+0.47}_{-0.09} M_\odot$
Radiated energy $E_{\rm rad}$	$> 0.025 M_\odot c^2$	$> 0.025 M_\odot c^2$
Luminosity distance $D_{\rm L}$	40^{+8}_{-14} Mpc	40^{+8}_{-14} Mpc
Viewing angle Θ	$\leq 55°$	$\leq 56°$
Using NGC 4993 location	$\leq 28°$	$\leq 28°$
Combined dimensionless tidal deformability $\tilde{\Lambda}$	≤ 800	≤ 700
Dimensionless tidal deformability $\Lambda(1.4 M_\odot)$	≤ 800	≤ 1400

Tidal Effects and Equation of State of Nuclear Material

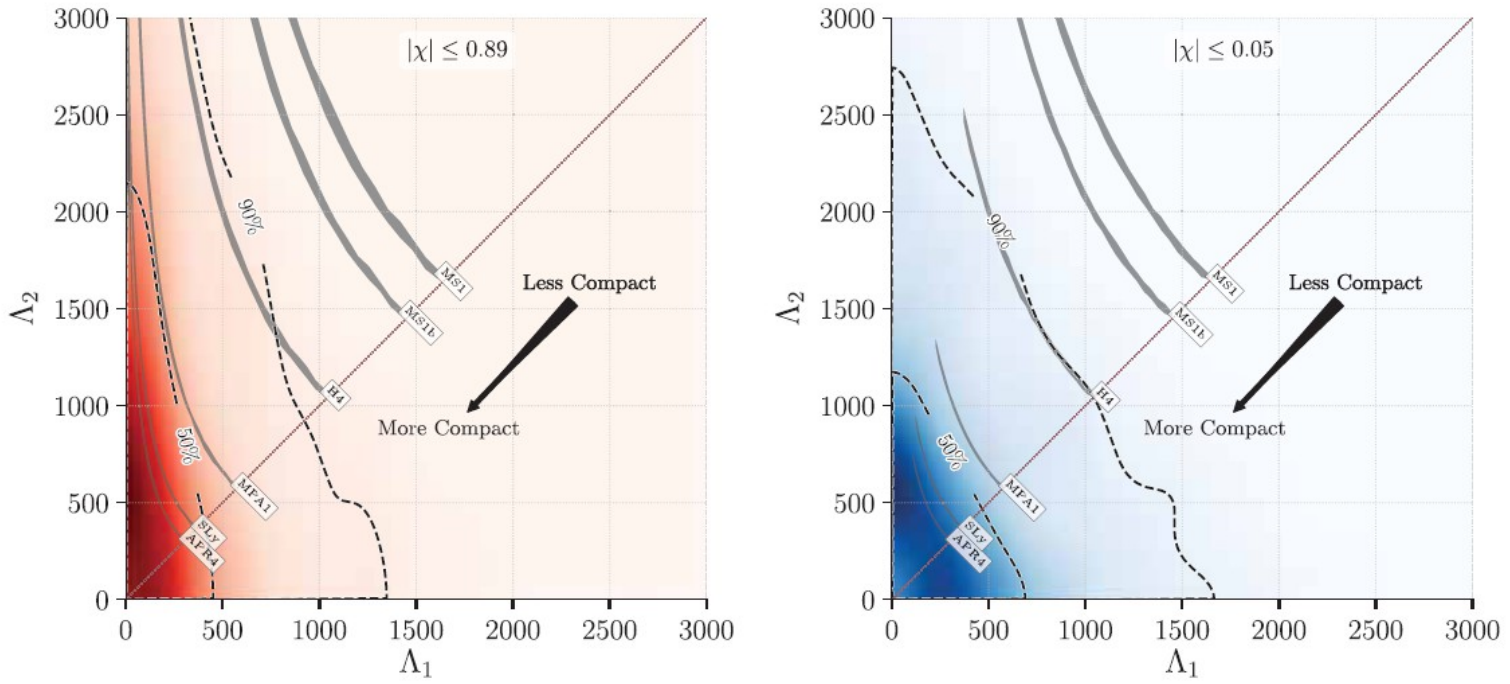

FIG. 5. Probability density for the tidal deformability parameters of the high and low mass components inferred from the detected signals using the post-Newtonian model. Contours enclosing 90% and 50% of the probability density are overlaid (dashed lines). The diagonal dashed line indicates the $\Lambda_1 = \Lambda_2$ boundary. The Λ_1 and Λ_2 parameters characterize the size of the tidally induced mass deformations of each star and are proportional to $k_2(R/m)^5$. Constraints are shown for the high-spin scenario $|\chi| \leq 0.89$ (left panel) and for the low-spin $|\chi| \leq 0.05$ (right panel). As a comparison, we plot predictions for tidal deformability given by a set of representative equations of state [156–160] (shaded filled regions), with labels following [161], all of which support stars of $2.01M_\odot$. Under the assumption that both components are neutron stars, we apply the function $\Lambda(m)$ prescribed by that equation of state to the 90% most probable region of the component mass posterior distributions shown in Fig. 4. EOS that produce less compact stars, such as MS1 and MS1b, predict Λ values outside our 90% contour.

Implications for a Stochastic Background

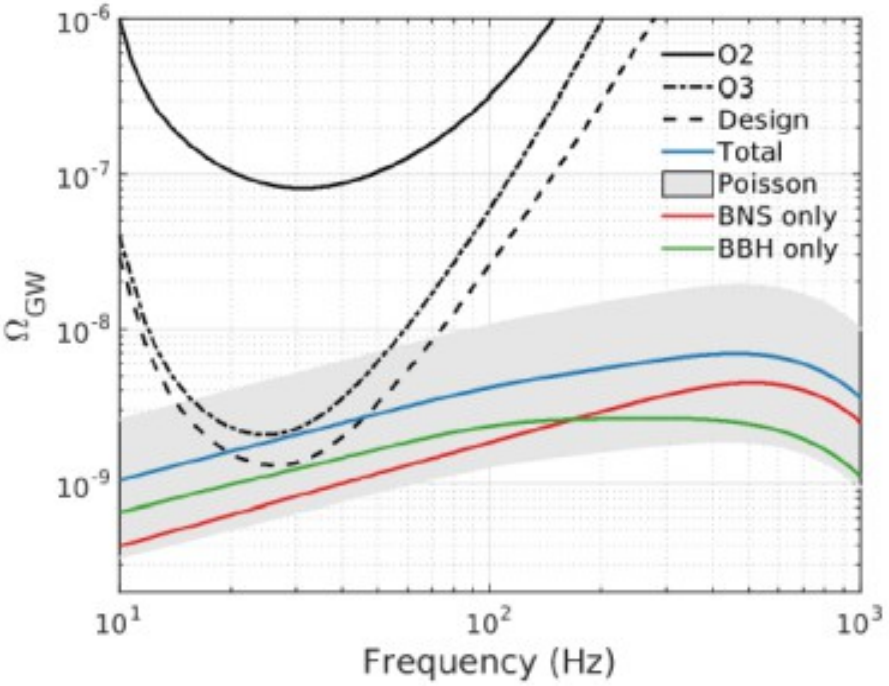

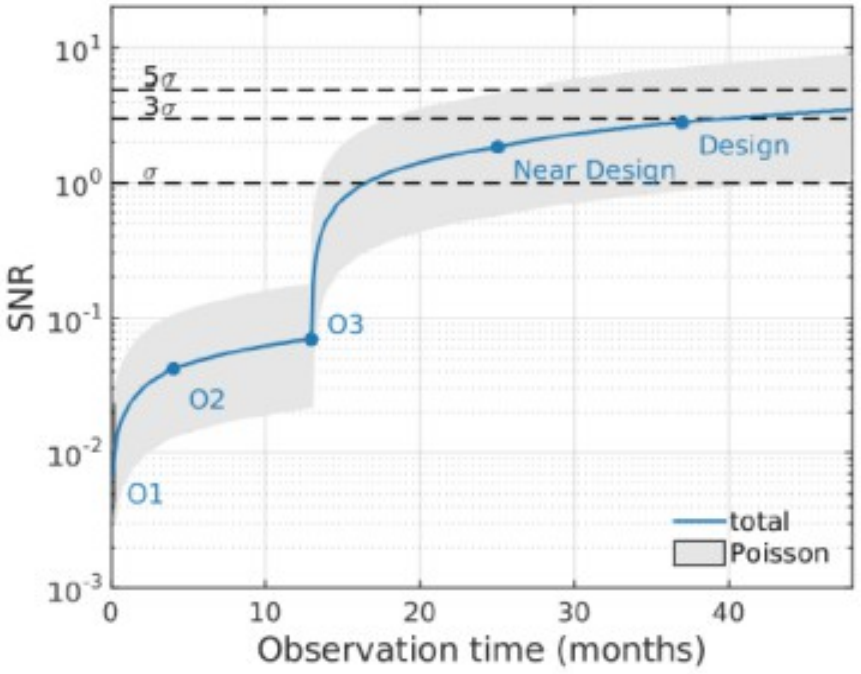

"Assuming the most probable rate for compact binary mergers, we find that the total background may be detectable with a signal to-noise-ratio of 3 after 40 months of total observation time."

T. Regimbau

Submitted PRL

New Test of the Equivalence Principle

$$\delta t_{\rm S} = -\frac{1+\gamma}{c^3}\int_{\mathbf{r}_{\rm e}}^{\mathbf{r}_{\rm o}} U(\mathbf{r}(l))dl$$

δt_S = Shapiro delay using the same time bounds

$\mathbf{r_o}$ = observation positon, $\mathbf{r_e}$ = emission position

$U(\mathbf{r})$ = gravitational potential (here the Milky Way's)

= wave path

γ = deviation from Einstein-Maxwell theory (where γ_{EM} and γ_{GW} are both equal to 1)

$$-2.6\times10^{-7} \leq \gamma_{\rm GW} - \gamma_{\rm EM} \leq 1.2\times10^{-6}$$

The best absolute bound on $\gamma_{\rm EM}$ is $\gamma_{\rm EM}-1 = (2.1\pm2.3)\times10^{-5}$, from the measurement of the Shapiro delay (at radio wavelengths) with the Cassini spacecraft (Bertotti et al. 2003).

Olivier Minazzoli

The Speed of Gravity

$$\Delta v = v_{\rm GW} - v_{\rm EM}$$

$$\Delta v / v_{\rm EM} \approx v_{\rm EM} \Delta t / D$$

$$-3 \times 10^{-15} \leq \frac{\Delta v}{v_{\rm EM}} \leq +7 \times 10^{-16}$$

Assuming D = 26 Mpc (the lower bound on the 90% confidence interval for distance based on GW data alone, and bounding t between [-10, +1.74] s, where the -10 s is a reasonably conservative assumption.

Gamma Rays with Fermi GBM

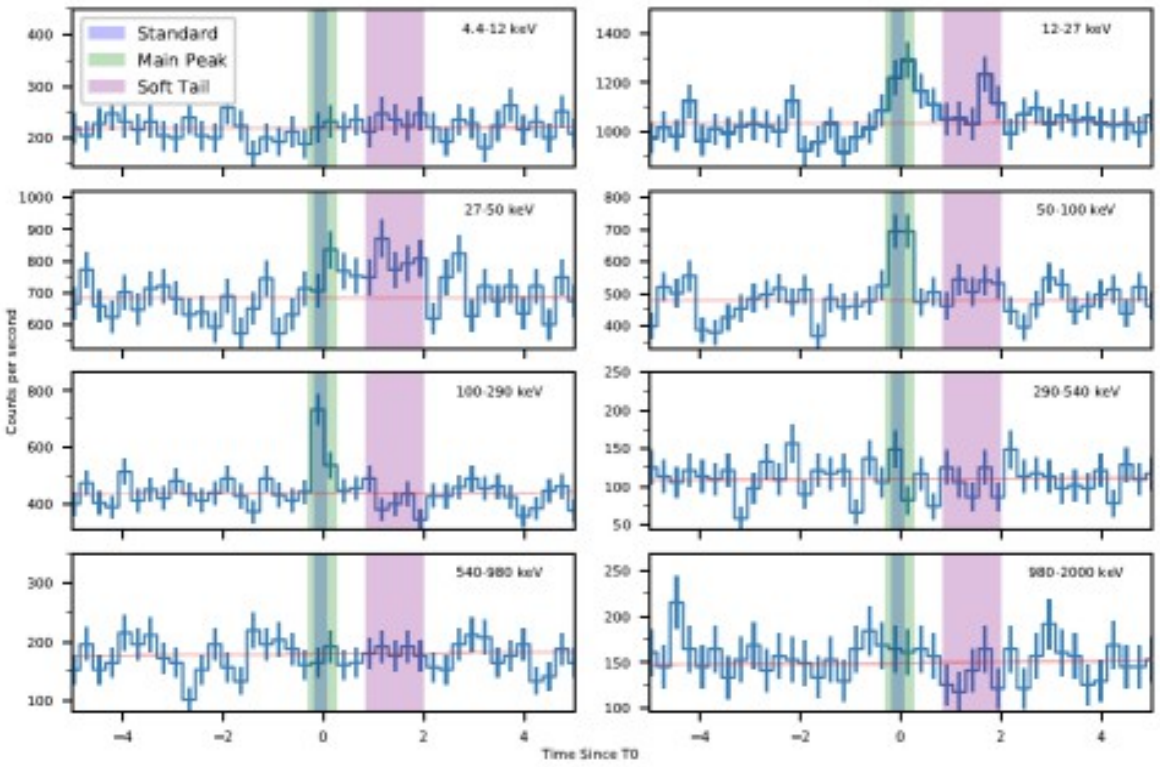

Figure 6. The 256 ms binned lightcurve of GRB 170817A for NaI 1, 2, and 5 over the standard 8 CTIME energy channels. The shaded regions are the different time intervals selected for spectral analysis. The inclusion of the lower energies shows the soft tail out to T0+2 s.

Two components: Main peak 0.5s and a soft tail ~2s

GRB 170817A – Very Dim

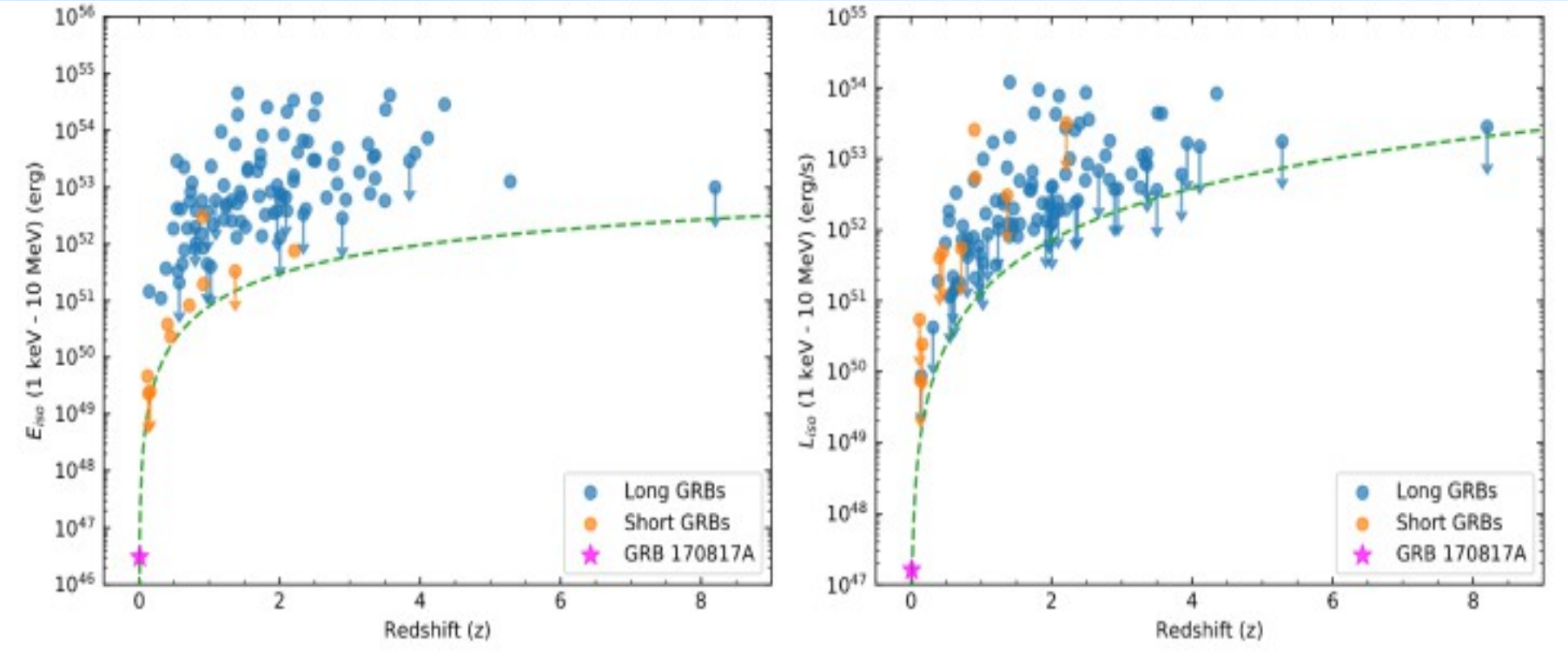

GRB 170716A is 2 to 6 orders of magnitude less energetic than previously known sGRBs with firm redshifts.

Future Observing Runs

Living Rev. Relativity, **19**, (2016), 1
DOI 10.1007/lrr-2016-1

LIVING REVIEWS in relativity

Prospects for Observing and Localizing Gravitational-Wave Transients with Advanced LIGO and Advanced Virgo

Abbott, B. P. et al.
The LIGO Scientific Collaboration and the Virgo Collaboration
(The full author list and affiliations are given at the end of paper.)
email: lsc-spokesperson@ligo.org, virgo-spokesperson@ego-gw.it

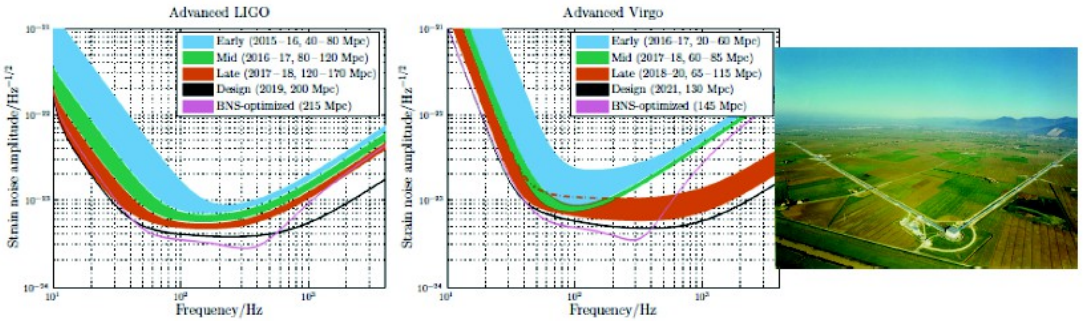

Figure 1: aLIGO (*left*) and AdV (*right*) target strain sensitivity as a function of frequency. The binary neutron-star (BNS) range, the average distance to which these signals could be detected, is given in megaparsec. Current notions of the progression of sensitivity are given for early, mid and late commissioning phases, as well as the final design sensitivity target and the BNS-optimized sensitivity. While both dates and sensitivity curves are subject to change, the overall progression represents our best current estimates.

2015–2016 (O1) A four-month run (beginning 18 September 2015 and ending 12 January 2016) with the two-detector H1L1 network at early aLIGO sensitivity (40–80 Mpc BNS range).

2016–2017 (O2) A six-month run with H1L1 at 80–120 Mpc and V1 at 20–60 Mpc.

2017–2018 (O3) A nine-month run with H1L1 at 120–170 Mpc and V1 at 60–85 Mpc.

2019+ Three-detector network with H1L1 at full sensitivity of 200 Mpc and V1 at 65–115 Mpc.

O2 30-11-2016. to 25-8-2017. O3 in fall of 2018, if all goes well.

Expected Advanced LIGO-Virgo Sensitivities

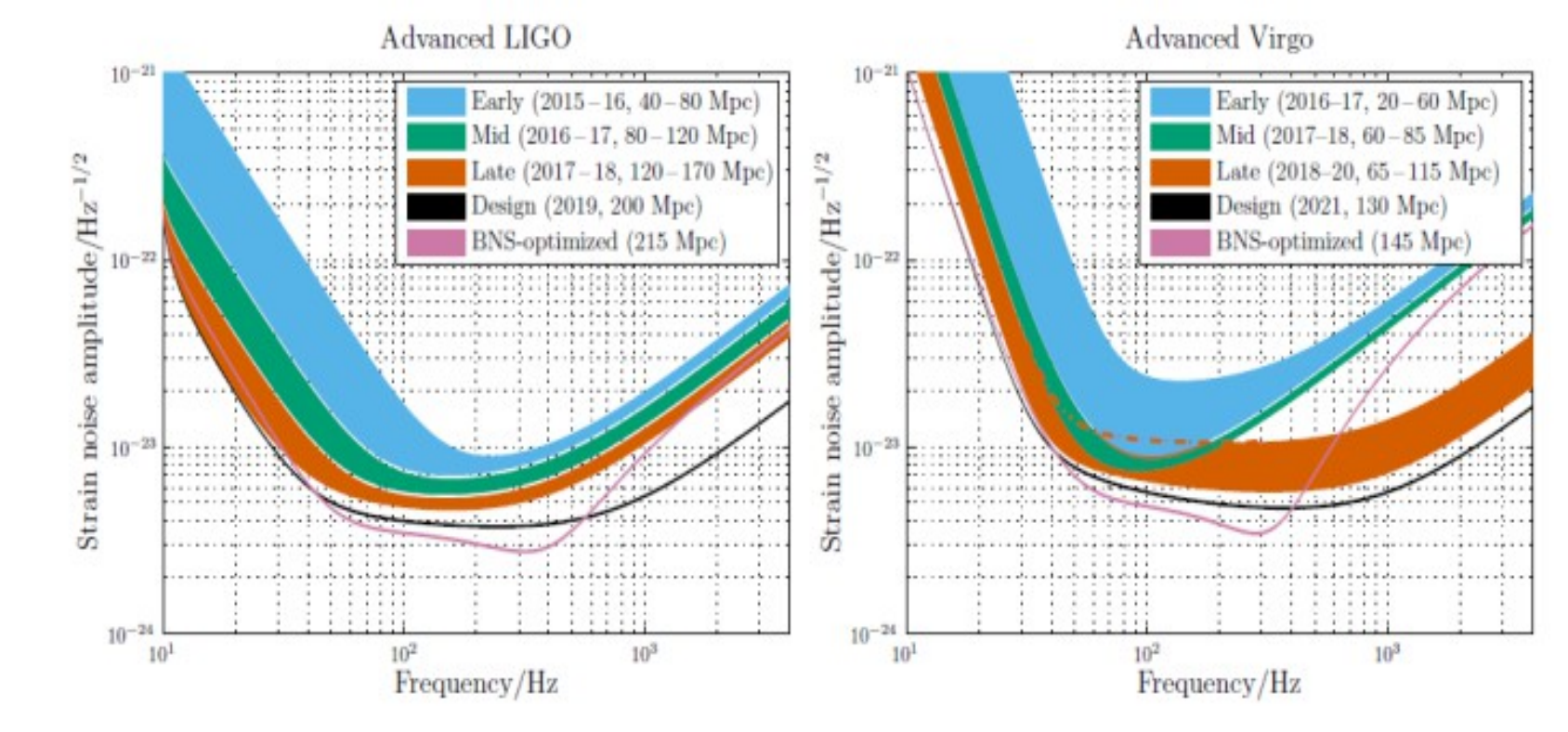

Living Rev. Relativity, **19**, (2016), 1
DOI 10.1007/lrr-2016-1

A detector network

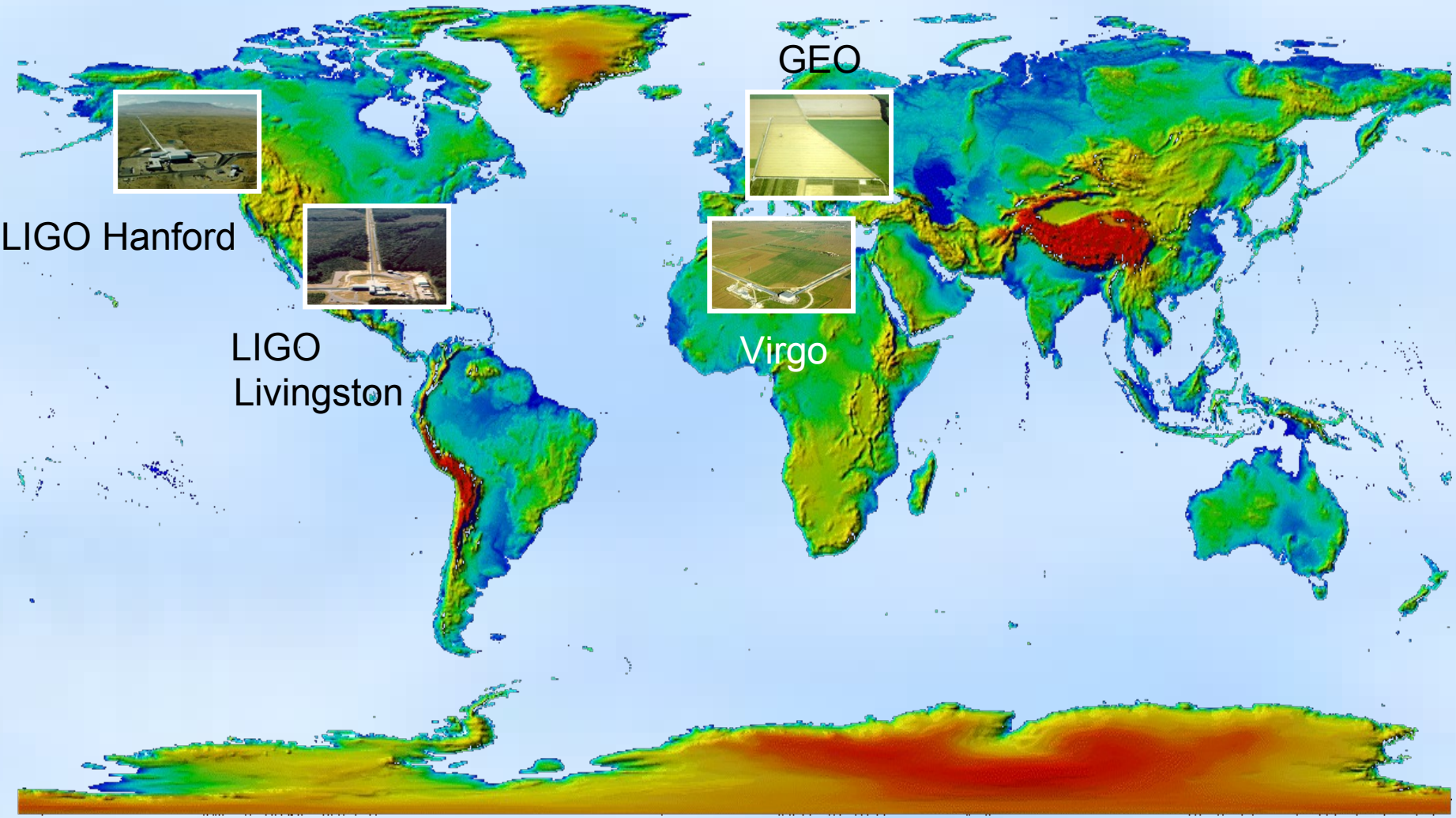

An even better detector network

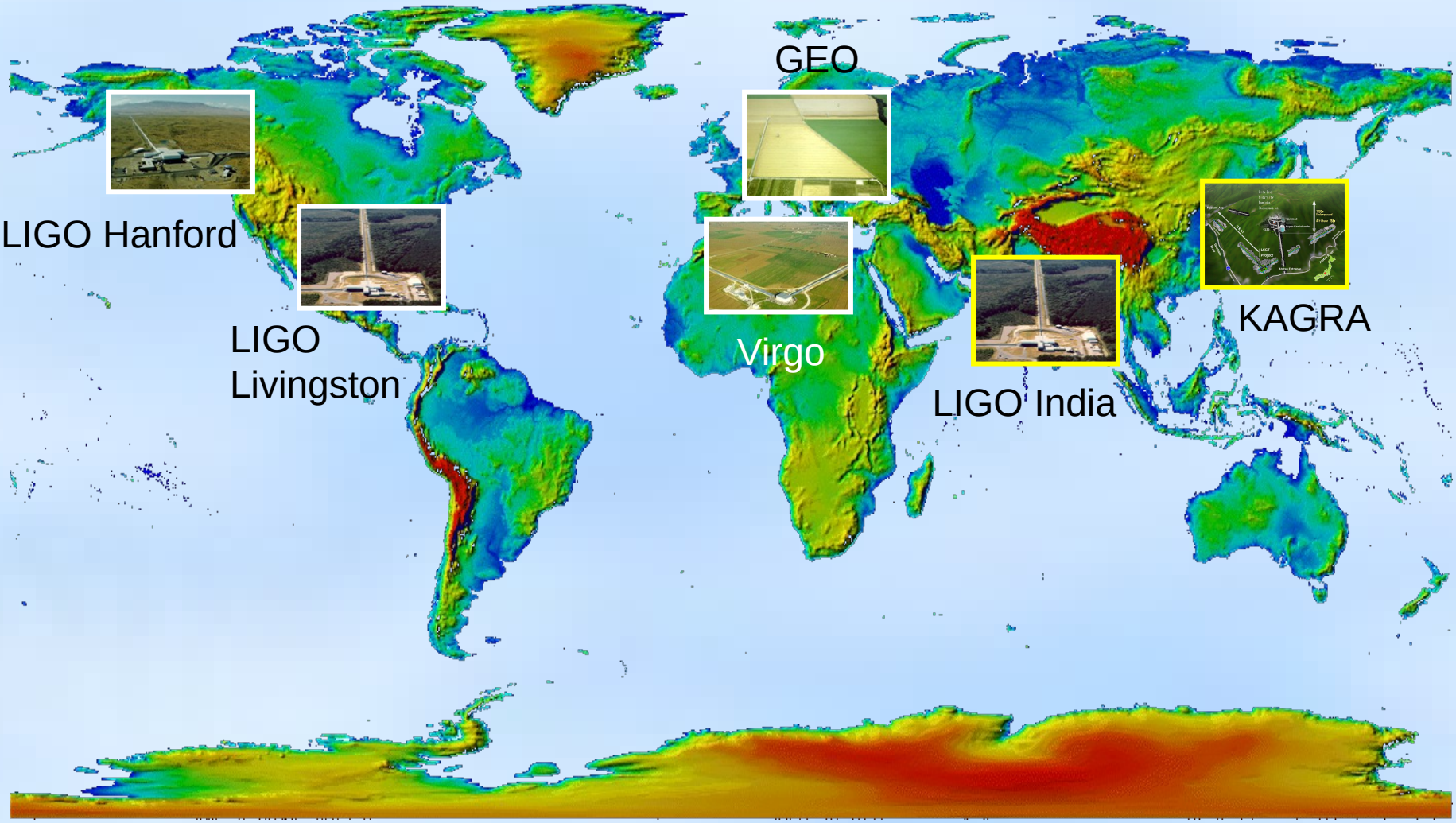

Advanced LIGO/Virgo sky localization

BNS source @ 80 Mpc

2016-2017 runs

2018-2019 runs

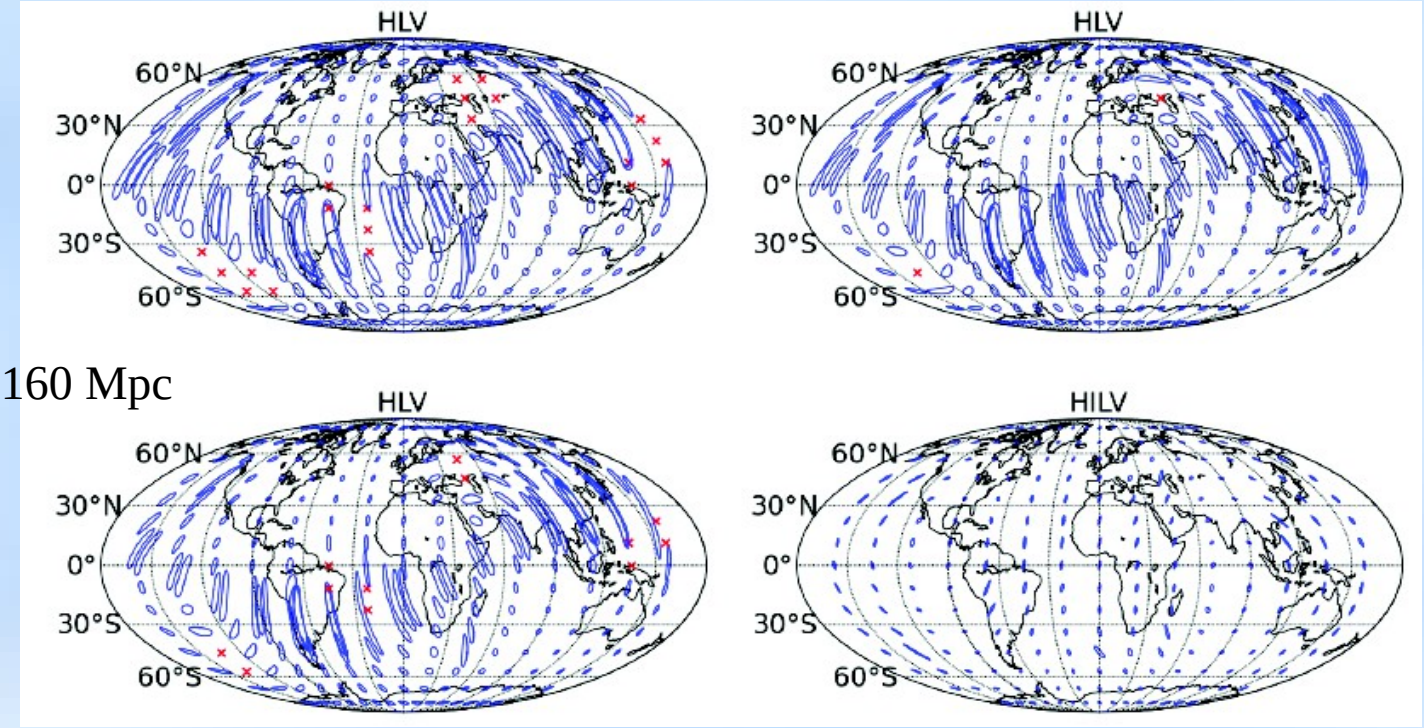

BNS source @ 160 Mpc

2019+ runs

HLV + LIGO India 2024+

Living Rev. Relativity, **19**, (2016), 1
DOI 10.1007/lrr-2016-1

LIGO – Virgo Summary

- Gravitational waves have been observed: black holes and neutron stars
- The universe has more stellar mass black holes than expected
- Mult-messenger astronomy has started!
- Observing run O2 is just completed. Virgo joined and made detections!
- KAGRA and LIGO-India will join in the coming years
- The future looks bright for ground based detectors